IRF8 Transcription-Factor-Dependent Classical Dendritic Cells Are Essential for Intestinal T Cell Homeostasis

Luda, Katarzyna M.; Joeris, Thorsten; Persson, Emma K.; Rivollier, Aymeric Marie Christian; Demiri, Mimoza; Sitnik, Katarzyna Maria; Pool, Lieneke; Holm, Jacob B.; Melo-Gonzalez, F.; Richter, Lisa

Total number of authors:
16

Published in:
Immunity

Link to article, DOI:
10.1016/j.immuni.2016.02.008

Publication date:
2016

Document Version
Publisher's PDF, also known as Version of record

Article

Immunity

IRF8 Transcription-Factor-Dependent Classical Dendritic Cells Are Essential for Intestinal T Cell Homeostasis

Graphical Abstract

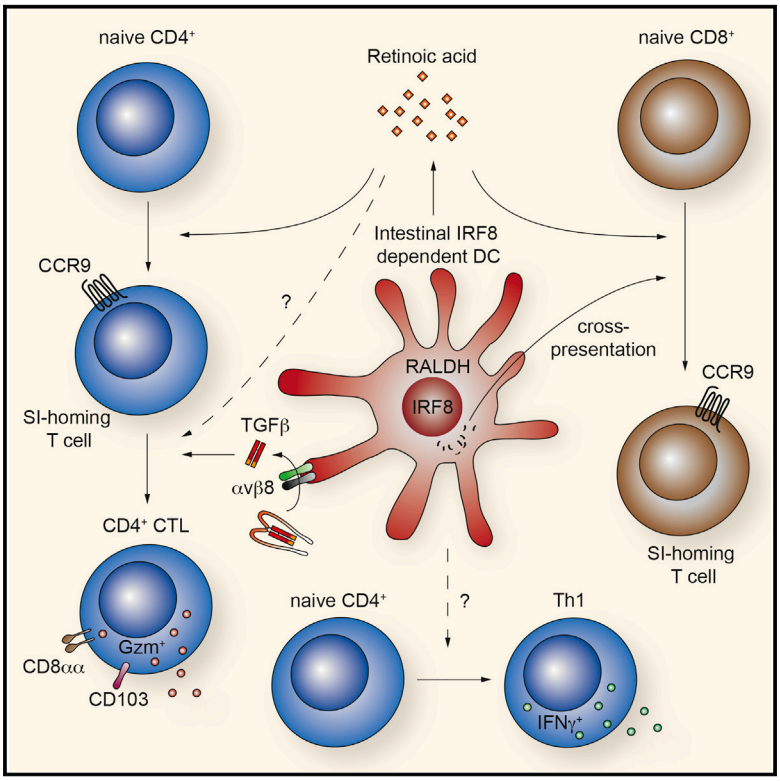

Highlights

- SI T cell numbers are reduced in the absence of IRF8-dependent DCs
- CD103^{+}CD11b^{-} migratory DCs are required for optimal generation of SI homing T cells
- β8 integrin expression by CD103^{+}CD11b^{-} DCs promotes SI CD4^{+}CD8αα^{+} IEL generation
- IRF8-dependent DCs play a key role in intestinal Th1 cell differentiation

Authors

Katarzyna M. Luda, Thorsten Joeris, Emma K. Persson, ..., Marcus Svensson-Frej, Knut Kotarsky, William W. Agace

Correspondence

william.agace@med.lu.se

In Brief

Classical dendritic are central regulators of adaptive immune responses. Here Agace and colleagues demonstrate multiple roles for IRF8 transcription factor-dependent classical DCs in intestinal adaptive immune homeostasis.

Luda et al., 2016, Immunity *44*, 1–15
April 19, 2016
http://dx.doi.org/10.1016/j.immuni.2016.02.008

CellPress

Please cite this article in press as: Luda et al., IRF8 Transcription-Factor-Dependent Classical Dendritic Cells Are Essential for Intestinal T Cell Homeostasis, Immunity (2016), http://dx.doi.org/10.1016/j.immuni.2016.02.008

IRF8 Transcription-Factor-Dependent Classical Dendritic Cells Are Essential for Intestinal T Cell Homeostasis

Katarzyna M. Luda,[1] Thorsten Joeris,[2] Emma K. Persson,[1,9] Aymeric Rivollier,[2] Mimoza Demiri,[1] Katarzyna M. Sitnik,[2] Lieneke Pool,[2] Jacob B. Holm,[3] Felipe Melo-Gonzalez,[4,5,6] Lisa Richter,[7] Bart N. Lambrecht,[8] Karsten Kristiansen,[3] Mark A. Travis,[4,5,6] Marcus Svensson-Frej,[1] Knut Kotarsky,[1] and William W. Agace[1,2,*]

[1]Immunology Section, Lund University, Lund 221 84, Sweden
[2]Section for Immunology and Vaccinology, National Veterinary Institute, Technical University of Denmark, 1870 Frederiksberg C, Denmark
[3]Laboratory of Genomics and Molecular Biomedicine, Department of Biology, University of Copenhagen, 2100 Copenhagen, Denmark
[4]Manchester Collaborative Centre of Inflammation Research (MCCIR), University of Manchester, Manchester M13 9NT, UK
[5]Wellcome Trust Centre for Cell-Matrix Research, University of Manchester, Manchester M13 9PT, UK
[6]Manchester Immunology Group, Faculty of Life Sciences, University of Manchester, Manchester M13 9PT, UK
[7]Centre for Immune Regulation and Department of Pathology, Oslo University Hospital – Rikshospitalet and University of Oslo, 0027 Oslo, Norway
[8]Inflammation Research Center (IRC), VIB-UGent Department, 9052 Ghent, Belgium
[9]Present address, Inflammation Research Center (IRC), VIB-UGent Department, 9052 Ghent, Belgium
*Correspondence: william.agace@med.lu.se
http://dx.doi.org/10.1016/j.immuni.2016.02.008

SUMMARY

The role of dendritic cells (DCs) in intestinal immune homeostasis remains incompletely defined. Here we show that mice lacking IRF8 transcription-factor-dependent DCs had reduced numbers of T cells in the small intestine (SI), but not large intestine (LI), including an almost complete absence of SI CD8$\alpha\beta^+$ and CD4$^+$CD8$\alpha\alpha^+$ T cells; the latter requiring β8 integrin expression by migratory IRF8 dependent CD103$^+$CD11b$^-$ DCs. SI homing receptor induction was impaired during T cell priming in mesenteric lymph nodes (MLN), which correlated with a reduction in aldehyde dehydrogenase activity by SI-derived MLN DCs, and inefficient T cell localization to the SI. These mice also lacked intestinal T helper 1 (Th1) cells, and failed to support Th1 cell differentiation in MLN and mount Th1 cell responses to *Trichuris muris* infection. Collectively these results highlight multiple non-redundant roles for IRF8 dependent DCs in the maintenance of intestinal T cell homeostasis.

INTRODUCTION

The intestinal mucosa contains a diverse array of T cells that play an essential role in maintaining tissue homeostasis, protection from mucosal pathogens and, when inadequately controlled, in driving immune pathology. Deciphering the key cellular and molecular pathways regulating the differentiation and maintenance of intestinal T cell subsets is thus essential to our understanding of mucosal immune homeostasis and disease and for the generation of more effective vaccines.

Intestinal T cells are diffusely distributed throughout the intestinal lamina propria (LP) and epithelium and collectively make up the largest populations of T cells in the body (Cheroutre and Madakamutil, 2004; Mowat and Agace, 2014). LP T cells consist primarily of CD4$^+$ T cells, which enter the intestine following activation in secondary lymphoid organs and might reside within the LP for long periods of time as tissue-resident memory (Trm) cells (Turner and Farber, 2014). They are functionally heterogeneous and include distinct subsets of interleukin-17 (IL-17)-producing T helper 17 (Th17) cells, interferon-γ (IFN-γ)-producing T helper 1 (Th1) cells, and diverse populations of regulatory T cells (Tregs) (Mowat and Agace, 2014). In contrast, small intestinal (SI) intraepithelial lymphocytes (IEL) can be broadly divided into two groups; "unconventional" CD8$\alpha\alpha^+$TCR$\alpha\beta^+$ and CD8$\alpha\alpha^+$TCR$\gamma\delta^+$ IEL and conventional CD8$\alpha\beta^+$TCR$\alpha\beta^+$ and CD4$^+$TCR$\alpha\beta^+$ IEL (Cheroutre et al., 2011). Like LP T cells, conventional IEL derive from lymphoid tissue primed T cells (Cheroutre et al., 2011) and might remain in the epithelium as Trm cells (Cauley and Lefrançois, 2013).

Intestinal dendritic cells (DCs) are located throughout the intestinal LP, in gut-associated lymphoid tissues (GALT), including Peyer's patches (PP) and solitary isolated lymphoid tissues, and in intestinal draining mesenteric lymph nodes (MLN). In addition to LN resident interferon regulatory factor (IRF) 8 and basic leucine zipper transcription factor ARF-like 3 (Batf3) dependent CD8α^+ and IRF4 expressing CD11b$^+$ DCs (Aliberti et al., 2003; Edelson et al., 2010; Persson et al., 2013) MLNs contain a large population of LP-derived CD11c$^+$ MHCII^{hi} migratory DCs that play a key role in the transport and presentation of intestinal derived self and foreign antigen (Huang et al., 2000; Jaensson et al., 2008; Schulz et al., 2009). The majority of DCs in the SI-LP (Johansson-Lindbom et al., 2005), and intestinal draining steady-state lymph (Cerovic et al., 2013; Schulz et al., 2009) express the integrin α_E(CD103)β_7 and can be divided into two major subsets; a Batf3- and IRF8-dependent subset of CD103$^+$CD11b$^-$ DCs

Please cite this article in press as: Luda et al., IRF8 Transcription-Factor-Dependent Classical Dendritic Cells Are Essential for Intestinal T Cell Homeostasis, Immunity (2016), http://dx.doi.org/10.1016/j.immuni.2016.02.008

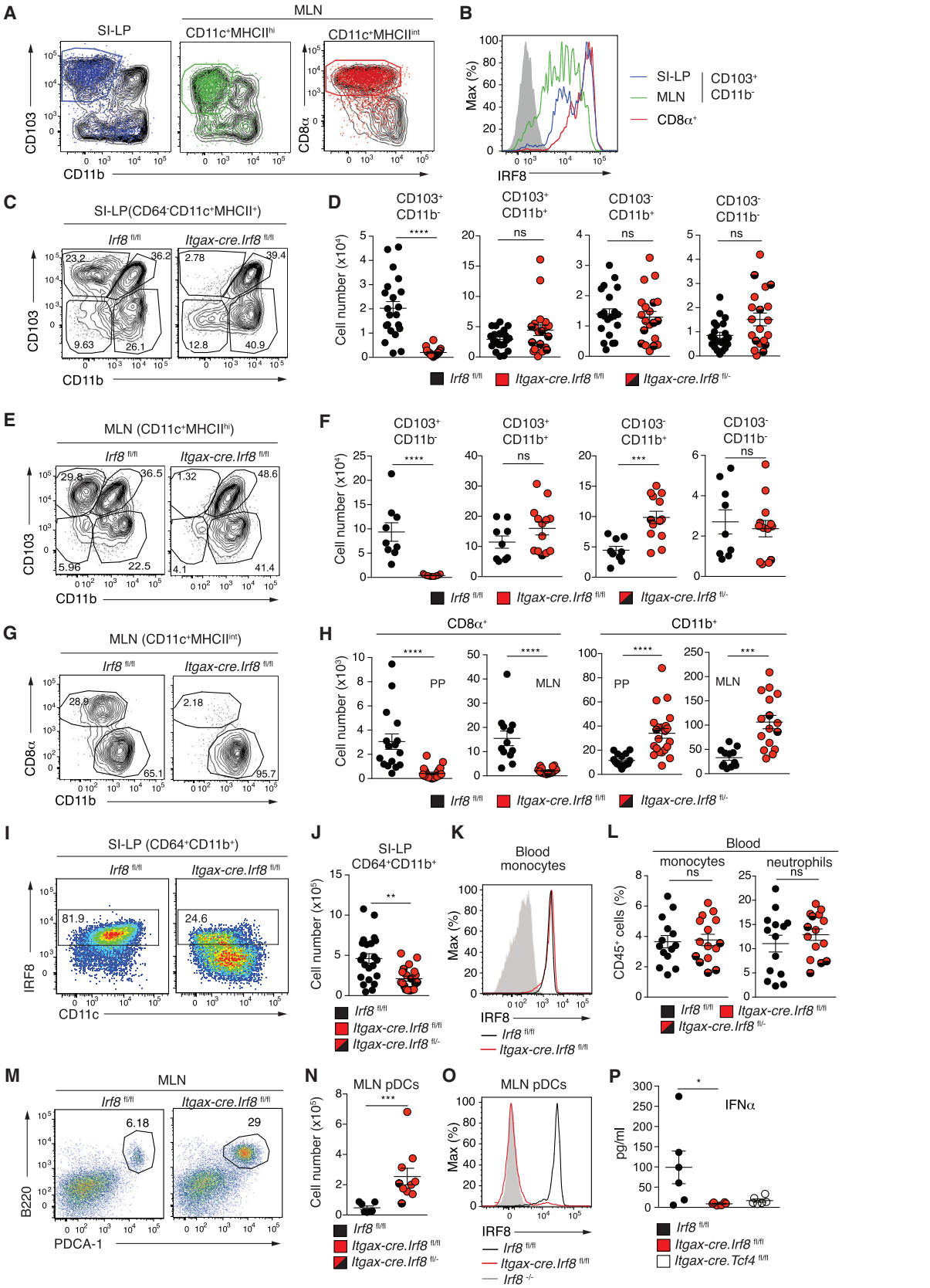

(legend on next page)

(Edelson et al., 2010), and an IRF4- and Notch2-dependent subset of CD103$^+$CD11b$^+$ DCs (Lewis et al., 2011; Persson et al., 2013). We, and others, have recently demonstrated that IRF4-dependent DCs have a non-redundant role in driving mucosal Th17 cell and Th2 cell responses (Gao et al., 2013; Persson et al., 2013; Schlitzer et al., 2013). In contrast, although IRF8-dependent DCs are recognized for their capacity to cross-present antigen (Shortman and Heath, 2010), and more recently to serve as a platform for CD4$^+$ T cell dependent CD8$^+$ T cell responses (Eickhoff et al., 2015; Hor et al., 2015), their role in the regulation of intestinal T cell homeostasis remains unknown.

RESULTS

IRF8 Deletion in CD11c$^+$ Cells Leads to a Loss in LN Resident CD8α^+ and Intestinal CD103$^+$CD11b$^-$ DCs

To explore the role of IRF8-dependent DCs in intestinal homeostasis, we initially assessed IRF8 expression in intestinal DC subsets by intracellular flow cytometry analysis. In the SI-LP, IRF8 was expressed by CD103$^+$CD11b$^-$ DCs and a minor subset of CD103$^-$ DCs (Figure 1A). In the MLN, IRF8 was expressed by lymph node resident CD8α^+MHCII^{int} DCs (Figures 1A and 1B) and SI-LP derived CD103$^+$CD11b$^-$ MHCII^{hi} DCs (Figures 1A and 1B). MLN resident CD8α^+MHCII^{int} DCs and SI-LP CD103$^+$CD11b$^-$ DCs expressed higher amounts of IRF8 than SI-LP derived CD103$^+$CD11b$^-$ DCs in the MLN (Figure 1B), suggesting that IRF8 expression is downregulated upon emigration from the intestine. To assess the role of IRF8 in intestinal DC homeostasis, we crossed *Itgax-cre* mice (Caton et al., 2007) with *Irf8*$^{fl/fl}$ mice. Germline deletion of *Irf8* occurred in a small proportion of offspring and we thus tracked the presence of the deleted and floxed *Irf8* allele in all pups. Quantitative genotyping and further analysis of the *Irf8* locus in these mice can be found in Supplemental Information and Figures S1A and S1B. IRF8 protein was not detected in CD11c$^+$MHCII$^+$ splenic or MLN cells from *Itgax-cre.Irf8*$^{fl/fl}$ and *Itgax-cre.Irf8*$^{fl/-}$ mice (Figure S1C and data not shown) consistent with efficient removal of the flox *Irf8* allele in these cells (Figure S1B). Because *Itgax-cre.Irf8*$^{fl/fl}$ and *Itgax-cre.Irf8*$^{fl/-}$ mice displayed similar phenotypes, data from these groups were pooled throughout. *Itgax-cre.Irf8*$^{fl/fl\ or\ fl/-}$ mice lacked CD103$^+$CD11b$^-$ DCs in the SI-LP, LI-LP, and MLN, while the numbers of SI-LP and LI-LP CD103$^-$ and SI-LP CD103$^+$CD11b$^+$ DCs were similar to those observed in *Irf8*$^{fl/fl}$ mice (Figures 1C–1F, Figures S2A and S2B). Consistent with previous findings in IRF8-deficient mice (Aliberti et al., 2003), *Itgax-cre.Irf8*$^{fl/fl\ or\ fl/-}$ mice lacked resident CD8α^+ DCs in Peyer's patch (PP), MLN, and the spleen (Figures 1G and 1H, and Figures S2C and S2D); these tissues also had enhanced numbers of resident CD11b$^+$ DCs (Figure 1H, and Figure S2D). As recently observed in *Irf8*$^{WT/-}$ mice (Grajales-Reyes et al., 2015), *Irf8*$^{fl/-}$ and *Itgax-cre.Irf8*$^{fl/WT}$ mice showed a major reduction in LN resident CD8α^+ DCs (Figures S2E and S2F), with unaltered numbers of migratory CD103$^+$CD11b$^-$ DC (Figures S2E and S2F), indicating differential gene dosage requirements between these populations.

IRF8-deficient mice have reduced numbers of circulating Ly6C^{hi} monocytes (Kurotaki et al., 2013), which can act as precursors of intestinal macrophages (Bain et al., 2014), and increased numbers of circulating neutrophils (Holtschke et al., 1996). We thus assessed whether IRF8 expression and numbers of these cells was altered in *Itgax-cre.Irf8*$^{fl/fl\ or\ fl/-}$ mice. IRF8 was expressed in SI-LP CD64$^+$CD11b$^+$ cells and circulating Ly6C^{hi} monocytes, but not in neutrophils (Figures 1I and 1K, Figure S1C), and in *Itgax-cre.Irf8*$^{fl/fl}$ mice IRF8 was deleted in SI-LP CD64$^+$CD11b$^+$ cells expressing the highest amounts of CD11c but not in Ly6C^{hi} monocytes (Figures 1I and 1K). The number of SI-LP CD64$^+$CD11b$^+$ cells was reduced in *Itgax-cre.Irf8*$^{fl/fl\ or\ fl/-}$ mice compared with *Irf8*$^{fl/fl}$ mice; however, the proportion of circulating Ly6C^{hi} monocytes and neutrophils was unchanged (Figures 1J and 1L). While the total number of splenic CD64$^+$ and CD64$^+$F4/80$^+$ myeloid cells was unaltered in *Itgax-cre.Irf8*$^{fl/fl\ or\ fl/-}$ mice (Figures S2G and S2H), there was a slight yet significant increase in splenic CD64$^+$CD11b$^+$ cells compared with *Irf8*$^{fl/fl}$ mice (Figure S2H).

While IRF8 is expressed by and required for the development of plasmacytoid DCs (pDCs) (Schiavoni et al., 2002), the total number of pDCs was increased in the MLN and spleen of *Itgax-cre.Irf8*$^{fl/fl\ or\ fl/-}$ mice compared with *Irf8*$^{fl/fl}$ mice (Figures 1M and 1N, and Figure S2I) despite an absence of IRF8 expression (Figure 1O). CD11c enriched splenic cells from *Itgax-cre.Irf8*$^{fl/fl}$ mice failed to produce IFNα after stimulation with D-type CpG-oligodeoxynucleotide 1585 (Figure 1P), a response that is pDC dependent (Kumagai et al., 2007) and absent in *Itgax-cre.Tcf4*$^{fl/fl}$ mice that display reduced numbers of pDCs (Cisse et al., 2008)(Figure 1P). Thus IRF8 is required for the regulation of pDC homeostasis and function.

Itgax-cre.Irf8$^{fl/fl\ or\ fl/-}$ Mice Have Reduced Numbers of SI-IEL

Next we assessed the impact of IRF8 deficiency in CD11c$^+$ cells on the composition and number of SI-IEL (Figure 2). The total number of CD45$^+$ cells was dramatically reduced in the SI epithelium of

Figure 1. Impact of IRF8 Deletion on Intestinal Mononuclear Phagocyte Subset Composition

(A) Representative flow cytometry plots of SI-LP and MLN DC subsets in C57BL/6 mice. Colored dots in each panel represent IRF8-expressing cells. Cells are pre-gated on live, CD45$^+$ Lin(CD19, B220, NK1.1, TER119)$^-$CD11c$^+$MHCII$^+$Ly6C$^-$CD64$^-$ cells.

(B) Intracellular IRF8 staining within the indicated gated DC populations in (A).

(C–H) Intestinal DC subset composition of *Itgax-cre.Irf8*$^{fl/fl\ or\ fl/-}$ and *Irf8*$^{fl/fl}$ mice. (C, E, G) Representative flow cytometry plots and (D, F, H) total cell number of (C) and (D) SI-LP, (E) and (F) MHCII^{hi} MLN DCs, and (G) and (H) MHCII^{int} MLN and PP DCs.

(I–O) (I, K, and O) Intracellular IRF8 staining, (J) and (N) total number or (L) frequency among CD45$^+$ cells of (I) and (J) SI-LP macrophages, (K) and (L) blood monocytes (Ly6G$^-$SiglecF$^-$CD64$^+$CD11b$^+$Ly6C^{hi}, left panel) and neutrophils (Ly6G$^+$CD11b$^+$SSC^{int}, right panel), and (N) and (O) MLN pDCs in *Itgax-cre.Irf8*$^{fl/fl\ or\ fl/-}$ and *Irf8*$^{fl/fl}$ littermates. (M) Representative flow cytometry plot of MLN pDCs. (K) FMO staining control (filled histogram).

(P) IFN-α production by MACS enriched splenic CD11c$^+$ cells from indicated mice following stimulation with CpG ODN 1585. Data are from (A, B, E, F, K, P) 2–4 or (C, D, G, H, I, J) 5–8 independent experiments. Each dot represents one mouse. Error bars represent mean ± SEM. *$p < 0.05$, **$p < 0.01$, ***$p < 0.001$, ****$p < 0.0001$, ns, not significant. See also Figure S1 and 2.

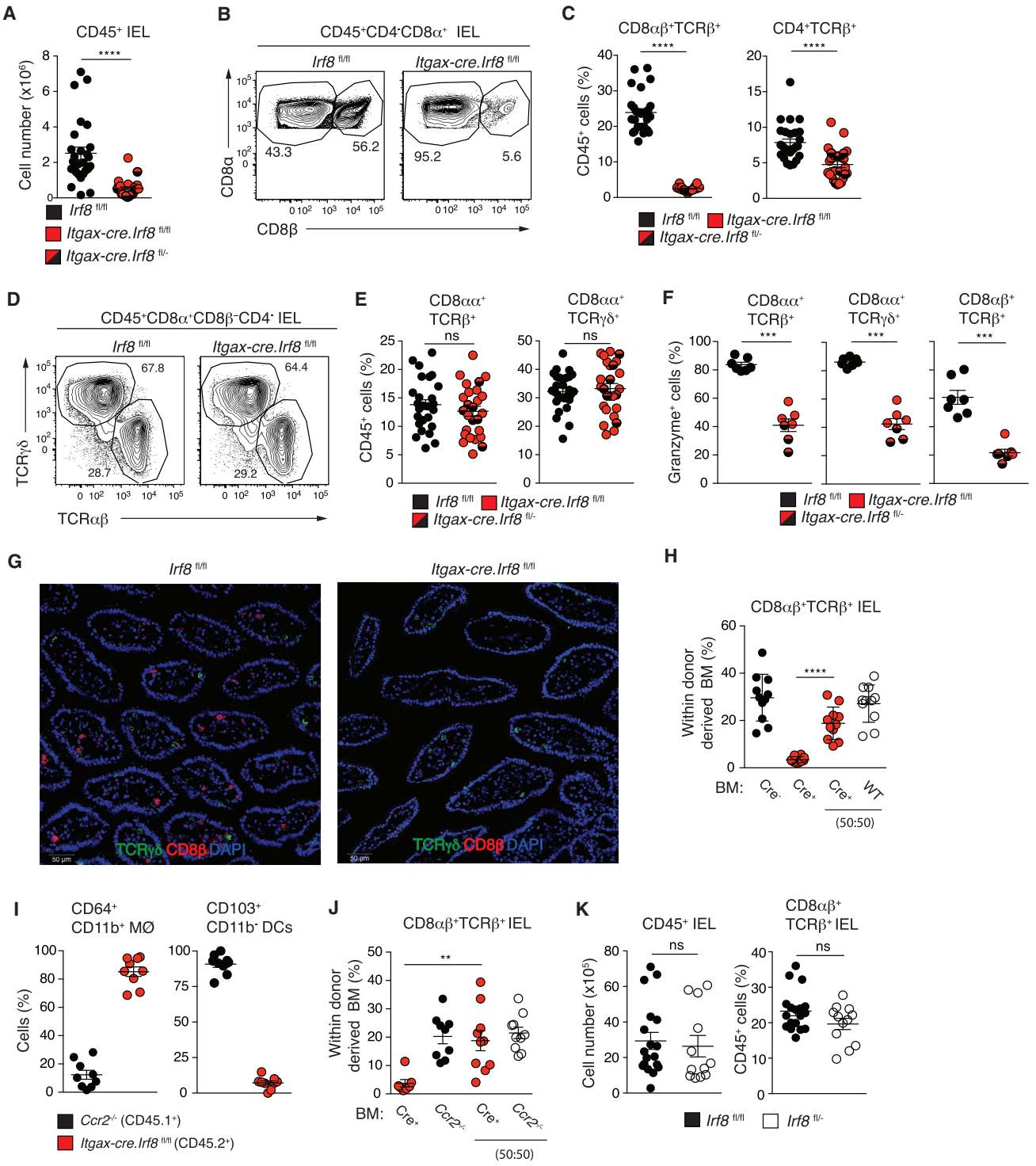

Figure 2. *Itgax-cre.Irf8* $^{fl/fl\ or\ fl/-}$ Mice Have Reduced Numbers of Conventional SI-IEL

(A–E) (A) Total number of CD45$^+$ cells IEL, (B) and (D) representative flow cytometry plots and (C) proportion of CD8αβ$^+$TCRβ$^+$, CD4$^+$TCRβ$^+$, and (E) CD8αα$^+$TCRβ$^+$ and CD8αα$^+$TCRγδ$^+$ among total CD45$^+$ SI-IELs in indicated mouse strains.

(F) Proportion of granzyme A$^+$ cells in indicated SI-IEL populations.

(G) Representative immunohistochemical staining of jejunum sections from indicated mice. DAPI, blue; TCRγδ, green; CD8β, red. Scale bar represents 50 μm.

(H) Percentage of CD8αβ$^+$ IEL within the indicated BM derived population in single and mixed BM chimeras.

(I) Percentage of SI-LP CD64$^+$CD11b$^+$ cells and CD103$^+$CD11b$^-$ MLN MHCII^{hi} DCs deriving from indicated BM from *Ccr2*$^{-/-}$.CD45.1$^+$:*Itgax-cre.Irf8*$^{fl/fl}$ mixed BM chimeras.

(legend continued on next page)

Itgax-cre.Irf8$^{fl/fl\ or\ fl/-}$ compared with *Irf8*$^{fl/fl}$ mice (Figure 2A) including an almost complete absence of CD8αβ$^+$TCRαβ$^+$ IEL together with a reduction in total CD4$^+$TCRαβ$^+$ IEL (Figures 2B and 2C, Figure S3A). *Itgax-cre.Irf8*$^{fl/fl\ or\ fl/-}$ mice also had significantly reduced numbers of CD8αα$^+$TCRαβ$^+$ and CD8αα$^+$TCRγδ$^+$ IEL (Figure S3A), although the proportion of CD8αα$^+$TCRαβ$^+$ and CD8αα$^+$TCRγδ$^+$IEL within CD45$^+$ IEL was similar to that of *Irf8*$^{fl/fl}$ mice (Figures 2D and 2E). Granzyme A expression was reduced in remaining CD8αβ$^+$TCRαβ$^+$, CD8αα$^+$TCRαβ$^+$, and CD8αα$^+$ TCRγδ$^+$ IEL in *Itgax-cre.Irf8*$^{fl/fl\ or\ fl/-}$ mice (Figure 2F). Analysis of intestinal sections confirmed an almost complete absence of SI CD8αβ$^+$ but not TCRγδ$^+$ IEL in *Itgax-cre.Irf8*$^{fl/fl}$ mice (Figure 2G). Such alterations in SI-IEL composition were not observed in *Itgax-cre.Irf4*$^{fl/fl\ or\ fl/-}$ mice (Figures S3B and S3C) that lack SI-LP derived CD103$^+$CD11b$^+$ MLN DCs (Persson et al., 2013).

Because SI-IEL can express CD11c (Huleatt and Lefrançois, 1995), and we detected both the flox and deleted *Irf8* allele in sorted splenic T cells from *Itgax-cre.Irf8*$^{fl/fl}$ mice (Figure S1C), we determined whether the reduction in conventional CD8αβ$^+$ IEL in *Itgax-cre.Irf8*$^{fl/fl}$ mice was a result of cell extrinsic or intrinsic effects by transferring a 1:1 ratio of BM from WT (CD45.1$^+$) and *Itgax-cre.Irf8*$^{fl/fl}$ (CD45.2$^+$) mice into WT (CD45.1$^+$CD45.2$^+$) recipients. Eight weeks after reconstitution, CD8αβ$^+$ IEL deriving from *Itgax-cre.Irf8*$^{fl/fl}$ BM were readily detected in the SI of the mixed BM chimeras (Figure 2H). Similar results were obtained in mixed *Rag1*$^{-/-}$ and *Itgax-cre.Irf8*$^{fl/fl}$ BM chimeras (data not shown). Thus the paucity of CD8αβ$^+$ IEL in *Itgax-cre.Irf8*$^{fl/fl}$ mice was primarily due to T and B cell extrinsic effects.

Because *Irf8* was deleted in a proportion of SI-LP CD64$^+$ CD11b$^+$ myeloid cells in *Itgax-cre.Irf8*$^{fl/fl\ or\ fl/-}$ mice (Figure 1I), we next assessed whether the reduction in CD8αβ$^+$ IEL might be related to IRF8 deficiency in CD64$^+$ cells. To this end, mixed BM chimeras were established by transferring a 1:1 ratio of BM from *Itgax-cre.Irf8*$^{fl/fl}$ (CD45.2$^+$) and *Ccr2*$^{-/-}$(CD45.1$^+$) mice, on the basis that *Ccr2*$^{-/-}$ BM would fail to re-establish IRF8 sufficient intestinal CD64$^+$ cells (Bain et al., 2014). Indeed, analysis of mixed BM chimeras 8 weeks after reconstitution demonstrated that almost all CD64$^+$ cells in the SI-LP derived from *Itgax-cre.Irf8*$^{fl/fl}$ BM whereas migratory CD103$^+$CD11b$^-$ DCs and CD8α$^+$ resident DCs in the MLN derived from *Ccr2*$^{-/-}$ BM (Figure 2I and data not shown). *Itgax-cre.Irf8*$^{fl/fl}$ BM was capable of generating CD8αβ$^+$ IEL in these mixed BM chimeras and granzyme A expression was restored in all subsets of SI-IEL derived from *Itgax-cre.Irf8*$^{fl/fl}$ BM (Figure 2J and data not shown). These results suggest that alterations in SI-IEL composition in *Itgax-cre.Irf8*$^{fl/fl}$ mice is not due to a loss of IRF8 expression in SI-LP CD64$^+$ cells. Further *Irf8*$^{fl/-}$ and *Itgax-cre.Tcf4*$^{fl/fl}$ mice had normal numbers and composition of SI-IEL (Figure 2K, Figures S3D and S3E), suggesting that LN resident CD8α$^+$ DCs and functional pDCs are not critical for maintenance of SI-IEL homeostasis. Collectively these results suggest an important role for intestinal CD103$^+$CD11b$^-$ DCs in intestinal IEL homeostasis.

Itgax-cre.Irf8$^{fl/fl\ or\ fl/-}$ Mice Display Deficiencies in Cross-Presenting Intraperitoneally Injected Soluble and Cellular Antigen

Given the marked reduction of CD8αβ$^+$ IEL in *Itgax-cre.Irf8*$^{fl/fl\ or\ fl/-}$ mice, we assessed the ability of *Itgax-cre.Irf8*$^{fl/fl\ or\ fl/-}$ and *Irf8*$^{fl/fl}$ mice to mount CD8$^+$ T cell responses to cell-associated and soluble antigen in vivo (Figure S4). Briefly, CellTrace Violet (VCT)-labeled OVA-specific CD8$^+$ (OT-I) T cells were injected intravenously (i.v.) into *Itgax-cre.Irf8*$^{fl/fl\ or\ fl/-}$ and *Irf8*$^{fl/fl}$ mice, recipient mice were immunized intraperitoneally (i.p.) with OVA or heat treated H-2^{bm1} MEFs expressing truncated non-secreted OVA (OVA-MEF, (Sancho et al., 2009)), and OT-I cell proliferation was assessed in the MLN and spleen 3 days later by flow cytometry. The sphingosine 1-phosphate receptor agonist FTY720 was administered i.p. to prevent effector lymphocyte egress from LN. OT-I responses to soluble OVA or OVA-MEF was markedly reduced in *Itgax-cre.Irf8*$^{fl/fl\ or\ fl/-}$ mice compared to *Irf8*$^{fl/fl}$ mice (Figures S4A and S4B). Consistent with these findings, while endogenous CD8$^+$ T cell numbers were unaffected in the MLN, or marginally lower in the spleen of *Itgax-cre.Irf8*$^{fl/fl\ or\ fl/-}$ mice, effector (CD62L$^-$CD44$^+$) CD8$^+$ T cell numbers were markedly reduced in both locations (Figure S4C). In contrast the total number of endogenous CD4$^+$ T cells in the MLN and spleen as well as the number of effector CD4$^+$ T cells in the MLN did not differ between *Itgax-cre.Irf8*$^{fl/fl\ or\ fl/-}$ and *Irf8*$^{fl/fl}$ mice (Figure S4C). Thus IRF8-dependent DCs play a non-redundant role in cross-presenting i.p. injected cell-associated and soluble antigen to CD8$^+$ T cells in vivo.

T Cells Primed in Intestinal Inductive Sites of *Itgax-cre.Irf8*$^{fl/fl\ or\ fl/-}$ Mice Have a Reduced Capacity to Localize to the Small Intestine

While a reduced cross-presenting capacity of *Itgax-cre.Irf8*$^{fl/fl}$ mice could in part underlie the dramatic reduction in CD8αβ$^+$ T cells in the SI epithelium and LP (Figure 3A), CD8αβ$^+$ T cell numbers were similar in the LI-LP and lung of *Itgax-cre.Irf8*$^{fl/fl\ or\ fl/-}$ and *Irf8*$^{fl/fl}$ mice (Figure 3A). Moreover, CD4$^+$ T cell numbers were reduced in the SI (Figure 2C and Figure 3A) but not LI-LP or lung of *Itgax-cre.Irf8*$^{fl/fl\ or\ fl/-}$ mice (Figure 3A and Figure S4C), indicating potential tissue specific defects regulating T cell accumulation in the SI. We therefore assessed the capacity of *Itgax-cre.Irf8*$^{fl/fl\ or\ fl/-}$ mice to support T cell priming after oral antigen administration and the subsequent migration of these cells to the SI. Briefly, VCT labeled OT-I or OVA specific CD4$^+$ (OT-II) T cells were injected i.v. into recipient *Itgax-cre.Irf8*$^{fl/fl\ or\ fl/-}$ or *Irf8*$^{fl/fl}$ mice and recipients were orally immunized with OVA with or without the TLR7 agonist R848. FTY720 was administered i.p. and the number and division history of responding donor T cells in MLN was assessed 3 (OT-I) and 4 (OT-II) days later (Figures 3B–3E). Following oral gavage of OVA OT-I cell numbers in the MLN of *Itgax-cre.Irf8*$^{fl/fl\ or\ fl/-}$ were lower than in *Irf8*$^{fl/fl}$ mice and these cells had undergone fewer divisions (Figures 3B and 3C), similar to responses after i.p. OVA administration (Figures S4A and SB). In contrast OT-I cells expanded equally efficiently in the MLN of *Itgax-cre.Irf8*$^{fl/fl\ or\ fl/-}$

(J) Percentage of CD8αβ$^+$ IEL within indicated BM derived CD45$^+$ population in single and mixed BM chimeras.
(K) Total number of CD45$^+$ IEL (left panel) and percentage of CD8αβ$^+$ IEL within CD45$^+$ IEL gate (right panel) in *Irf8*$^{fl/fl}$ and *Irf8*$^{fl/-}$ mice. Data are from (A, C, E) 9, (K) 6, or (B, D, F-J) 2–3 independent experiments performed. Each dot represents one mouse. Error bars represent mean ± SEM. *p < 0.05, **p < 0.01, ***p < 0.001, ****p < 0.0001, ns, not significant. See also Figure S3.

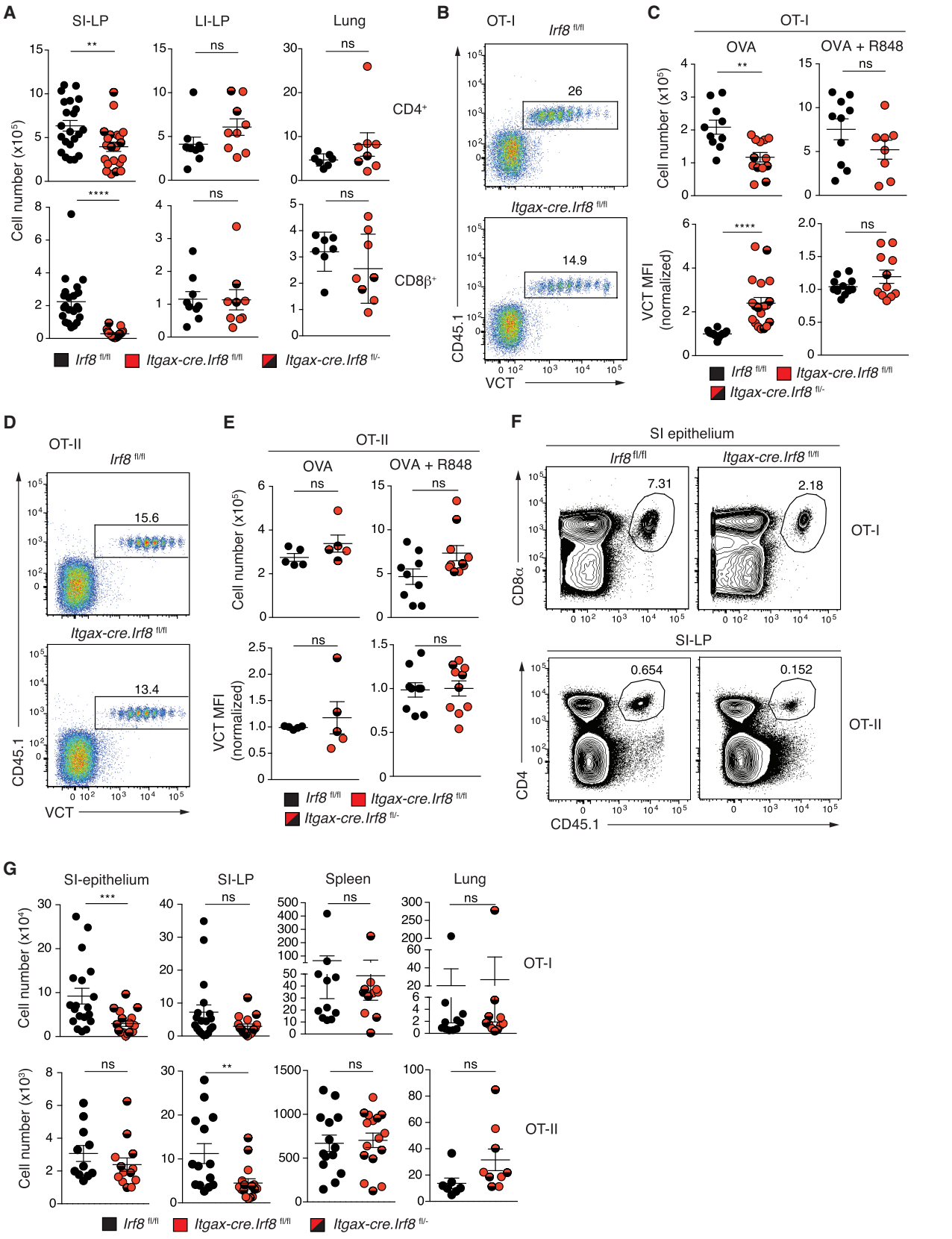

(legend on next page)

mice following oral administration of OVA and R848 (Figure 3C). OT-II cells proliferated equally well in *Itgax-cre.Irf8*$^{fl/fl\ or\ fl/-}$ and *Irf8*$^{fl/fl}$ mice in response to oral administration of OVA or OVA and R848 (Figures 3D and 3E). To assess whether effector T cells primed in *Itgax-cre.Irf8*$^{fl/fl\ or\ fl/-}$ mice were capable of localizing to the SI, we immunized OT-I or OT-II cell recipients orally with OVA and R848 (conditions of equal T cell proliferation) in the absence of FTY720 and their localization to the SI epithelium and LP assessed 4 days later by flow cytometry. OT-I cells primed in *Itgax-cre.Irf8*$^{fl/fl\ or\ fl/-}$ mice displayed a reduced ability to mobilize to the SI but not lung or spleen (Figures 3F and 3G) although this was only significant for the SI-epithelium (Figure 3G). OT-II numbers in general were low in the epithelium, consistent with the fact that most SI-IEL are CD8$^+$ T cells, however their accumulation in the SI-LP but not lung or spleen was significantly reduced in *Itgax-cre.Irf8*$^{fl/fl\ or\ fl/-}$ compared with *Irf8*$^{fl/fl}$ mice (Figure 3G).

T Cells Primed in the MLN of *Itgax-cre.Irf8*$^{fl/fl\ or\ fl/-}$ Mice Have Reduced CCR9 Expression

We hypothesized that *Itgax-cre.Irf8*$^{fl/fl\ or\ fl/-}$ mice might differ in their expression of the T cell homing receptor ligands CCL25 and MadCAM-1 in the SI, or that T cells primed in the MLN of these mice might be deficient in their expression of the SI homing receptors, CCR9 and $\alpha4\beta7$ (Agace, 2008). The proportion of CD31$^+$ PDPN$^-$ vascular endothelial cells expressing MadCAM-1 and the amount of *Ccl25* mRNA in the SI of *Itgax-cre.Irf8*$^{fl/fl\ or\ fl/-}$ mice were similar to that of *Irf8*$^{fl/fl}$ mice (Figures S5A and S5B) arguing against alterations in homing receptor ligand expression as a cause for reduced T cell localization to this site. To assess SI homing receptor induction, we determined CCR9 and $\alpha4\beta7$ expression on OT-I and OT-II cells in the MLN 3 (OT-I) and 4 (OT-II) days after oral administration of OVA or OVA and R848 and i.p. injection of FTY720 (Figure 4). In both situations, the proportion of OT-I and OT-II cells expressing CCR9, and the amount of CCR9 on CCR9-expressing cells was reduced in the MLN of *Itgax-cre.Irf8*$^{fl/fl\ or\ fl/-}$ compared with *Irf8*$^{fl/fl}$ mice (Figures 4A and 4B). The amount of $\alpha4\beta7$ on $\alpha4\beta7$ expressing cells was also reduced, although to a lesser extent (Figure 4C).

Induction of CCR9 and $\alpha4\beta7$ on T cells in vitro requires the vitamin A metabolite retinoic acid (RA) (Iwata et al., 2004; Svensson et al., 2008) and vitamin-A-deficient mice fail to support the generation of CCR9$^+\alpha4\beta7^+$ CD8$^+$ T cells in MLN in vivo (Jaensson-Gyllenbäck et al., 2011). Consistent with this reflecting a T cell intrinsic requirement for RA, CCR9 and $\alpha4\beta7$ were not induced after oral administration of OVA and R848 on adoptively transferred OT-I or OT-II cells that expressed a dominant negative form of the retinoic acid receptor α (RARα) (OT-I.*Cd4-cre.dnRara*$^{lsl/WT}$ or OT-II.*Cd4-Cre.dnRara*$^{lsl/WT}$) (Pino-Lagos et al., 2011)(Figure 4D). We thus hypothesized that T cells primed in the MLN of *Itgax-cre.Irf8*$^{fl/fl\ or\ fl/-}$ received less RA. Consistent with this possibility OT-I cells sorted from the MLN of recipient mice 3 days after oral OVA and R848 administration expressed lower amounts of the RA target gene *P2x7r* (Heiss et al., 2008) as well as *Ccr9* (Figure 4E).

The generation of CCR9$^+\alpha4\beta7^+$ T cells by intestinal DCs in vitro requires the activity of retinaldehyde dehydrogenases that convert retinal to retinoic acid (Iwata et al., 2004). We found that SI-LP derived CD103$^+$CD11b$^-$ DCs were significantly enriched in the fraction of MLN DCs displaying the highest aldehyde dehydrogenase (ALDH) activity (Yokota et al., 2009) (Figure 4F) and that MHCII^{hi} MLN DCs in *Itgax-cre.Irf8*$^{fl/fl\ or\ fl/-}$ mice displayed significantly reduced ALDH activity compared with *Irf8*$^{fl/fl}$ mice (Figure 4G). Collectively, these results suggest that RA production by IRF8-dependent CD103$^+$CD11b$^-$ migratory DCs is important for the optimal generation of SI homing T cells.

Itgax-cre.Irf8$^{fl/fl\ or\ fl/-}$ Mice Lack CD4$^+$CD8$\alpha\alpha^+$ IEL

Within the SI a subset of CD4$^+$TCR$\alpha\beta^+$ T cells differentiate into CD4$^+$CD8$\alpha\alpha^+$ IEL (Morrissey et al., 1995; Reimann and Rudolphi, 1995), a transition that is associated with induction of the cytotoxic T lymphocyte (CTL) associated runt-related transcription factor 3 (Runx3), and acquisition of MHC II restricted CTL like activity (Mucida et al., 2013; Reis et al., 2013). In addition to a reduction in total SI CD4$^+$TCR$\alpha\beta^+$ IEL (Figure 2C and Figure S3A), the CD4$^+$TCR$\alpha\beta^+$ IEL compartment of *Itgax-cre.Irf8*$^{fl/fl\ or\ fl/-}$ mice lacked CD4$^+$CD8$\alpha\alpha^+$ IEL (Figure 5A), expressing granzyme A (Figure 5B), and the NK and memory CD8$^+$ T cell marker CD244 (2B4) (Figure 5C) (Mucida et al., 2013). Among total SI CD4$^+$TCR$\alpha\beta^+$ IEL both CD4$^+$CD8$\alpha\alpha^+$ and, to a lesser extent, CD4$^+$CD8$\alpha\alpha^-$ IEL express CD103 (Figure 5D) (Reis et al., 2013); however, all CD4$^+$TCR$\alpha\beta^+$ IEL lacked CD103 expression in *Itgax-cre.Irf8*$^{fl/fl\ or\ fl/-}$ mice (Figure 5E). The percentage of CD8$\alpha\beta^+$TCRβ^+, CD8$\alpha\alpha^+$TCR$\gamma\delta^+$, and CD8$\alpha\alpha^+$TCR$\alpha\beta^+$ IEL expressing CD103, as well as the amount of CD103 expression by CD8$^+$CD103$^+$ IEL, were also significantly reduced in *Itgax-cre.Irf8*$^{fl/fl\ or\ fl/-}$ mice (Figure 5F and data not shown). Consistent with a lack of CD4$^+$CD8$\alpha\alpha^+$ IEL, remaining CD4$^+$TCR$\alpha\beta^+$ IEL in *Itgax-cre.Irf8*$^{fl/fl\ or\ fl/-}$ mice expressed lower amounts of *Cd8a*, *Cd244*, *Gzma*, *Gzmb*, and *Itgae* mRNA, as well as *Runx3* and *Tbx21* (encoding Tbet) (Figure 5G), a transcription factor associated with the transition of CD4$^+$ T cells into CD4$^+$CD8$\alpha\alpha^+$ IEL (Mucida et al., 2013; Reis et al., 2013). Lack of CD4$^+$CD8$\alpha\alpha^+$ IEL and reduced CD103 expression by CD4$^+$TCR$\alpha\beta^+$ IEL was T cell extrinsic as CD4$^+$CD8$\alpha\alpha^+$ IEL and CD103 expressing CD4$^+$TCR$\alpha\beta^+$ IEL were generated efficiently from *Itgax-cre.Irf8*$^{fl/fl}$ BM in WT (CD45.1$^+$):*Itgax-cre.Irf8*$^{fl/fl}$ (CD45.2$^+$) as well as *Rag1*$^{-/-}$:*Itgax-cre.Irf8*$^{fl/fl}$ mixed BM chimeras (Figure 5H, data not shown). Further, CD4$^+$CD8$\alpha\alpha^+$ IEL and CD103 expressing CD4$^+$TCR$\alpha\beta^+$ IEL deriving from *Itgax-cre.Irf8*$^{fl/fl}$ BM were readily

Figure 3. T Cells Primed in Intestinal Inductive Sites of *Itgax-cre.Irf8*$^{fl/fl\ or\ fl/-}$ Display a Reduced Capacity to Localize to the Small Intestine

(A) Total number of CD4$^+$ and CD8$\alpha\beta^+$ T cells in indicated organs of *Irf8*$^{fl/fl}$ and *Itgax-cre.Irf8*$^{fl/fl\ or\ fl/-}$ mice.

(B–E) (B) and (D) show representative flow cytometry plots and (C) and (E) show total number and division history of (B and C) OT-I and (D and E) OT-II cells in the MLN of indicated recipient mice (B and C) 3 and (D and E) 4 days after oral gavage with OVA or OVA and R848. MFI, median fluorescence intensity normalized to the median MFI value of the *Irf8*$^{fl/fl}$ group.

(F) Representative flow cytometry plots and (G) total number of OT-I and OT-II cells in the indicated organs 4 days after oral gavage with OVA and R848. Data are from 2–7 independent experiments. Each dot represents one mouse. Error bars represent mean ± SEM. *$p < 0.05$, **$p < 0.01$, ***$p < 0.001$, ****$p < 0.0001$, ns, not significant. See also Figure S4.

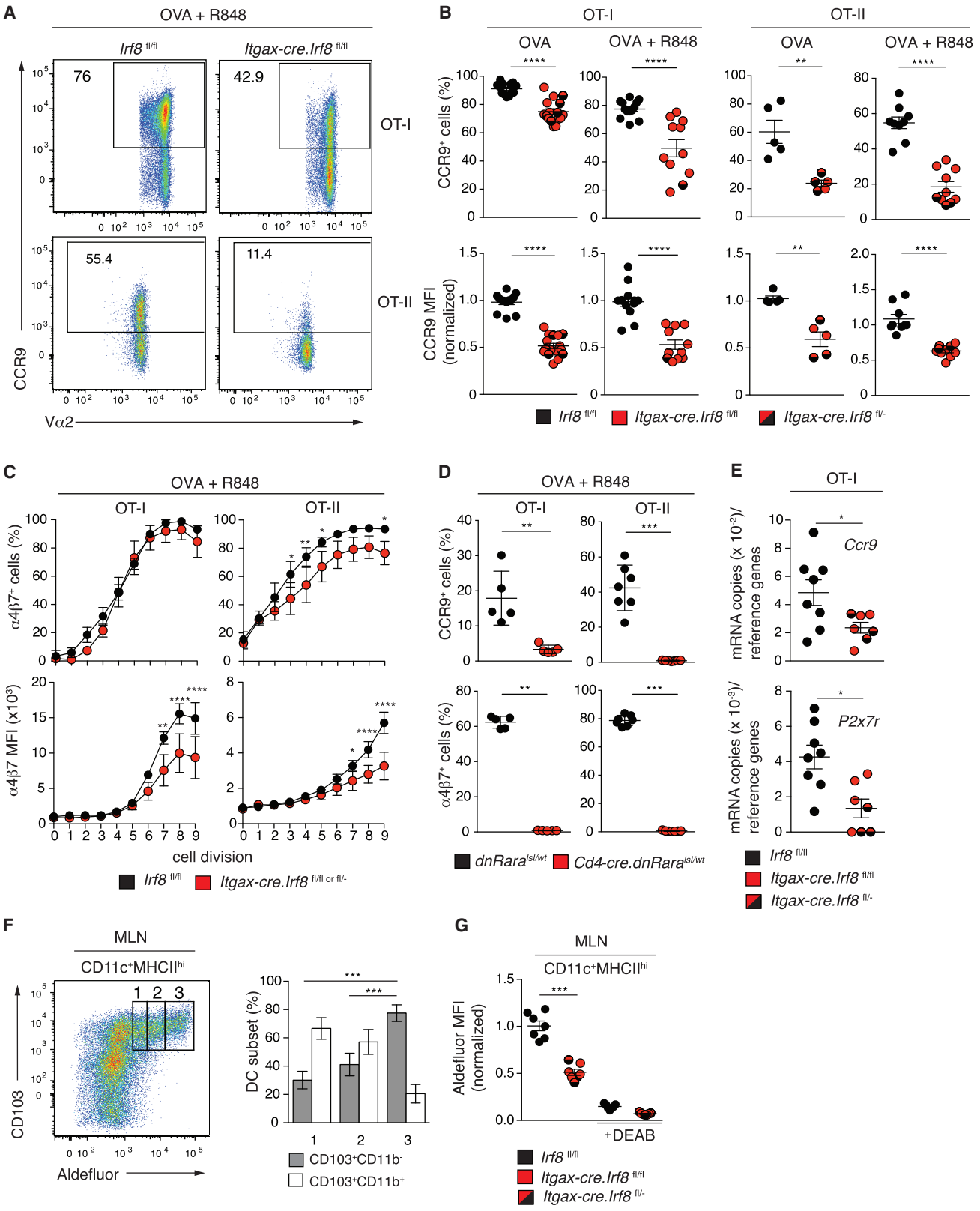

Figure 4. T Cells Primed in the MLN of *Itgax-cre.Irf8*$^{fl/fl\ or\ fl/-}$ Mice Have Reduced Expression of Small Intestinal Homing Receptors

(A) Representative flow cytometry plots and (B) pooled data of (A) and (B) CCR9 and (C) α4β7 expression on OT-I or OT-II cells in the MLN of indicated recipient mice 3 (OT-I) or 4 (OT-II) days after oral gavage with OVA or OVA and R848.

(legend continued on next page)

detected in *Ccr2*$^{-/-}$ (CD45.1$^+$):*Itgax-cre.Irf8*$^{fl/fl}$ (CD45.2$^+$) mixed BM chimeras (Figure 5I) and were present in normal numbers in *Itgax-cre.Tcf4*$^{fl/fl}$ mice (Figure S4F).

β8 Integrin Subunit Expression by IRF8 Dependent CD103$^+$CD11b$^-$ DCs Is Required for the Generation of CD4$^+$CD8αα$^+$ IEL

Because the differentiation of CD4$^+$TCRαβ$^+$ T cells to CD4$^+$ CD8αα$^+$ IEL and the induction of CD103 on intestinal IEL is TGF-β dependent (El-Asady et al., 2005; Reis et al., 2013), we next assessed the expression of genes involved in TGF-β production and activation in intestinal DC subsets. qPCR analysis demonstrated that *Itgb8*, encoding the β8 integrin chain involved in the activation of latent TGF-β (Travis and Sheppard, 2014), was expressed selectively by CD103$^+$CD11b$^-$ DCs (Figure 5J). To investigate the functional significance of β8 integrin expression by CD103$^+$CD11b$^-$ DCs in CD4$^+$CD8αα$^+$ IEL development, we generated *Itgax-cre.Itgb8*$^{fl/fl}$ mice. While displaying normal numbers of CD45$^+$ SI-IEL and proportions of CD4$^+$TCRαβ$^+$ SI-IEL (Figure 5K, data not shown), these animals had significantly reduced proportions of CD4$^+$CD8αα$^+$ IEL compared with *Itgb8*$^{fl/fl}$ littermates (Figure 5K, data not shown). Further BM from *Itgb8*$^{fl/fl}$, but not from *Itgax-cre.Itgb8*$^{fl/fl}$ mice rescued the generation of CD4$^+$CD8αα$^+$ SI-IEL and CD103 expression on CD4$^+$TCRαβ$^+$ SI-IEL in mixed BM chimeras with *Itgax-cre.Irf8*$^{fl/fl}$ BM (Figure 5L). Thus β8 integrin expression by IRF8-dependent DCs is required for the generation of CD4$^+$CD8αα$^+$ IEL.

Itgax-cre.Irf8$^{fl/fl\ or\ fl/-}$ Mice Lack Intestinal Th1 Cells

We next compared intestinal LP CD4$^+$ T cell subset composition in *Itgax-cre.Irf8*$^{fl/fl\ or\ fl/-}$ and *Irf8*$^{fl/fl}$ mice (Figures 6A and 6B). Strikingly, IFN-γ$^+$IL-17$^-$ CD4$^+$ T cells were almost absent and IFN-γ$^+$IL-17$^+$ CD4$^+$ T cells were reduced in the SI-LP and LI-LP of *Itgax-cre.Irf8*$^{fl/fl\ or\ fl/-}$ mice (Figures 6A and 6B). In contrast, *Itgax-cre.Irf8*$^{fl/fl\ or\ fl/-}$ mice had elevated proportions of intestinal IL-17$^+$IFN-γ$^-$ cells, while the proportions of Foxp3$^+$CD4$^+$ T cells were slightly reduced in the LI but not SI (Figures 6A and 6B). Consistent with these findings, SI-LP CD4$^+$ T cells from *Itgax-cre.Irf8*$^{fl/fl\ or\ fl/-}$ mice expressed lower amounts of *Tbx21,* but not *Rorc* or *Foxp3*, compared with *Irf8*$^{fl/fl}$ mice (Figures 6C). Naive splenic CD4$^+$ T cells from *Itgax-cre.Irf8*$^{fl/fl}$ and *Irf8*$^{fl/fl}$ mice differentiated equally well into IFN-γ producing Th1 cells in vitro (Figure 6D), and IFN-γ producing CD4$^+$ T cells deriving from *Itgax-cre.Irf8*$^{fl/fl}$ BM were present in the SI and MLN of WT (CD45.1$^+$):*Itgax-cre.Irf8*$^{fl/fl}$ (CD45.2$^+$) mixed BM chimeras (Figure 6E). Further, IFN-γ producing SI-LP CD4$^+$ T cells were readily detected in *Itgax-cre.Tcf4*$^{fl/fl}$ mice (Figure 6F). Despite these defects in mucosal T cell homeostasis, the composition of the cecal and colonic microbiota, including amounts of segmented filamentous bacteria, did not differ between *Itgax-cre.Irf8*$^{fl/fl\ or\ fl/-}$ and *Irf8*$^{fl/fl}$ mice (Figures S6A–S6D), and *Itgax-cre.Irf8*$^{fl/fl\ or\ fl/-}$ mice displayed no major defects in intestinal barrier function as assessed by amounts of serum endotoxin (Figure S6E).

Th1 Cell Differentiation Is Impaired in the MLN of *Itgax-cre.Irf8*$^{fl/fl\ or\ fl/-}$ Mice

To assess whether Th1 cell priming in MLN was altered in *Itgax-cre.Irf8*$^{fl/fl\ or\ fl/-}$ mice, OT-II cells were injected i.v. into *Itgax-cre.Irf8*$^{fl/fl\ or\ fl/-}$ and *Irf8*$^{fl/fl}$ mice and recipients were immunized with OVA, LPS, and αCD40 i.p., a protocol previously demonstrated to generate both IFN-γ and IL-17 producing OT-II populations (Persson et al., 2013). While OT-II cells primed in the MLN of both *Itgax-cre.Irf8*$^{fl/fl\ or\ fl/-}$ and *Irf8*$^{fl/fl}$ mice expressed IL-17 (Figures 7A and 7B), the MLN of *Itgax-cre.Irf8*$^{fl/fl\ or\ fl/-}$ mice failed to support Th1 cell differentiation (Figures 7A and 7B). *Ccr2*$^{-/-}$ mice, that displayed dramatically reduced numbers of CD64$^+$ CD11b$^+$ cells in the MLN 4 days after immunization (Figure 7C), supported efficient Th1 cell differentiation (Figure 7D), as did *Itgax-cre.Tcf4*$^{fl/fl}$ mice (Figure 7E). Finally, when *Itgax-cre.Irf8*$^{fl/fl\ or\ fl/-}$ and *Irf8*$^{fl/fl}$ mice were infected orally with 20 *Trichuris muris* (*T. muris*) eggs, a dose that drives a Th1 cell response resulting in chronic infection in C57BL/6 mice (Bancroft et al., 1994), chronic infection developed in *Irf8*$^{fl/fl}$ mice but not *Itgax-cre.Irf8*$^{fl/fl\ or\ fl/-}$ mice (Figure 7F). Further while both sets of mice generated an equivalent *T. muris* specific immunoglobulin G1 (IgG1) response, *Itgax-cre.Irf8*$^{fl/fl\ or\ fl/-}$ mice failed to mount a *T. muris*-specific IgG2c response (Figure 7G). Collectively, these findings suggest a role for IRF8-dependent DCs in the generation of intestinal Th1 cell responses and offer one likely mechanism underlying the dramatic reduction in Th1 cells in the SI-LP and LI-LP of *Itgax-cre.Irf8*$^{fl/fl\ or\ fl/-}$ mice.

DISCUSSION

Itgax-cre.Irf8$^{fl/fl\ or\ fl/-}$ mice displayed a similar reduction in classical DC subsets to that previously reported in *Irf8*$^{-/-}$ and *Irf8*^{R294C} mice (Aliberti et al., 2003; Edelson et al., 2010). However, in contrast to *Irf8*-deficient mice that lack pDCs (Schiavoni et al., 2002), *Itgax-cre.Irf8*$^{fl/fl\ or\ fl/-}$ mice had increased numbers of pDCs, although these appeared dysfunctional. *Irf8*^{R294C} mice have also been reported to have higher numbers of pDCs (Tailor et al., 2008), collectively indicating that distinct IRF8 interacting partners might be required for pDC development versus pDC homeostasis and functionality. Although it remains possible that dysfunctional IRF8-deficient pDCs influence SI T cell homeostasis, our findings provide evidence that it is primarily an absence of classical IRF8-dependent DCs that underlie the defects in intestinal T cell homeostasis observed in *Itgax-cre.Irf8*$^{fl/fl\ or\ fl/-}$ mice.

(D) CCR9 and α4β7 expression on OT-I and OT-II.*cd4-cre*. *dnRara*$^{lsl/WT}$ or *dnRara*$^{lsl/WT}$ cells in the MLN of recipient mice 3 (OT-I) or 4 (OT-II) days after oral gavage with OVA and R848.

(E) Relative expression of *Ccr9* and *P2x7r* on divided OT-I cells in the MLN of recipient mice 3 days after oral gavage with OVA and R848.

(F) and (G) ALDH activity of (F) MHCII^{hi} MLN DC subsets in *Irf8*$^{fl/fl}$ mice and (G) MHCII^{hi} MLN DC in *Irf8*$^{fl/fl}$ and *Itgax-cre.Irf8*$^{fl/fl\ or\ fl/-}$ mice. (F, left) Representative flow cytometry plot and (F, right) proportion of CD103$^+$CD11b$^-$ and CD103$^+$CD11b$^+$ DCs in the indicated gates in the left hand plot. (G) MFI, mean fluorescence intensity. DEAB (N,N-diethylaminobenzaldehyde, ALDH inhibitor). Data are from (A, B, E–G) 2–4 independent experiments or (C) a representative experiment of three performed or (D) one experiment. (B, D, E, G) Each dot represents one mouse, (C) pooled data from three mice per group. Error bars represent mean ± SEM, (F) mean ± SD. *p < 0.05, **p < 0.01, ***p < 0.001, ****p < 0.0001, ns, not significant. See also Figure S5.

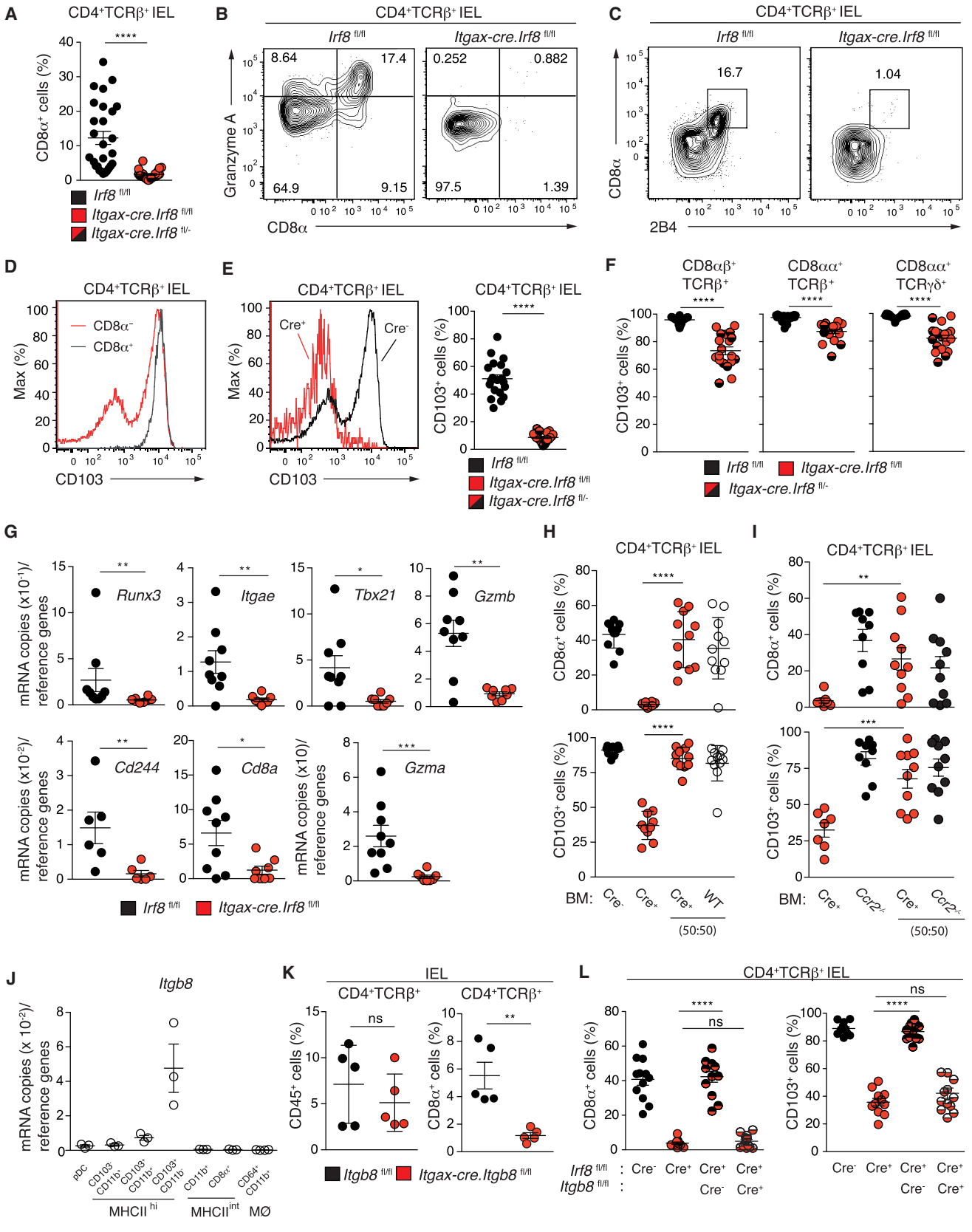

(legend on next page)

Our finding that *Irf8*$^{fl/-}$ mice had normal numbers of SI CD8αβ$^+$ T cells, despite a major reduction in LN resident CD8α$^+$ DCs, suggest that a lack of migratory CD103$^+$CD11b$^-$ DCs is responsible for the paucity of SI CD8αβ$^+$ T cells in *Itgax-cre.Irf8*$^{fl/fl\ or\ fl/-}$ mice. One likely contributing factor underlying this deficiency is the reduced capacity of *Itgax-cre.Irf8*$^{fl/fl\ or\ fl/-}$ mice to cross-present antigen. Nevertheless these mice had similar numbers of CD8αβ$^+$ T cells as controls in the LI and lung, indicating additional tissue specific mechanisms. In this regard, both CD4$^+$ and CD8$^+$ T cells primed in the MLN of *Itgax-cre.Irf8*$^{fl/fl\ or\ fl/-}$ mice had reduced expression of the SI homing receptor CCR9 and localized less efficiently to the SI but not lung. Although both SI-derived CD103$^+$CD11b$^+$ and CD103$^+$CD11b$^-$ DCs display retinaldehyde dehydrogenase activity (Cerovic et al., 2013; Denning et al., 2011; Persson et al., 2013), we here demonstrate that SI-derived CD103$^+$CD11b$^-$ DCs display the highest amounts of aldehyde dehydrogenase activity in MLN, and their absence in *Itgax-cre.Irf8*$^{fl/fl\ or\ fl/-}$ mice resulted in a decrease in DC-derived aldehyde dehydrogenase activity. We thus hypothesize that optimal generation of "SI tropic" T cells requires RA signals from CD103$^+$CD11b$^-$ DCs, potentially providing an additional explanation for the reduced numbers of SI CD8αβ$^+$ and SI CD4$^+$ T cells in *Itgax-cre.Irf8*$^{fl/fl\ or\ fl/-}$ mice. These results do not exclude the possibility that SI-derived CD103$^+$CD11b$^-$ DCs also support "SI tropic" T cell generation in the MLN through additional mechanisms. Notably, SI lymphoid tissues were also recently suggested to be sites of unconventional IEL precursor activation, associated with an enhanced expression of CCR9 and α4β7 (Guy-Grand et al., 2013). Whether a similar mechanism contributes to the reduction in unconventional IEL numbers or whether the development and maintenance of these cells is altered in *Itgax-cre.Irf8*$^{fl/fl\ or\ fl/-}$ mice await further study.

In addition to an overall reduction in SI CD4$^+$ T cell numbers CD4$^+$ IEL of *Itgax-cre.Irf8*$^{fl/fl\ or\ fl/-}$ mice failed to express CD103 and to differentiate into CD4$^+$CD8αα$^+$ IEL. These results are consistent with a recent study in *Batf3*$^{-/-}$ mice indicating an important role for cell adhesion molecule 1 (Cadm1) expression by Batf3 dependent DCs in driving CD4$^+$CD8αα$^+$ IEL generation (Cortez et al., 2014). Here we show that αvβ8 integrin expression by CD103$^+$CD11b$^-$ DCs also plays a key role in the generation of CD4$^+$CD8αα$^+$ IEL as well as in the induction of CD103 on CD4$^+$ IEL. Whether αvβ8 and Cadm1 function together or independently of one another to promote CD4$^+$CD8αα$^+$ IEL development remains to be determined.

Itgax-cre.Irf8$^{fl/fl\ or\ fl/-}$ mice had normal proportions of intestinal FoxP3$^+$ Treg cells, consistent with previous findings in *Batf3*$^{-/-}$ mice (Edelson et al., 2010) and increased proportions of intestinal IL-17$^+$IFN-γ$^-$ Th17 cells. This phenotype is markedly distinct from that of *Itgax-cre.Itgb8*$^{fl/fl}$ mice that have reduced numbers of colonic FoxP3$^+$ T cells and Th17 cells (Melton et al., 2010; Travis et al., 2007) suggesting that αvβ8 expression by a CD11c$^+$ cell distinct from IRF8-dependent DCs is required for intestinal Th17 cell homeostasis. Alternatively a complete absence of IRF8-dependent DCs might lead to the generation of additional αvβ8 independent signals that promote the generation of these cells. Given our previous work demonstrating reduced numbers of intestinal IL-17$^+$IFN-γ$^-$ Th17 cells in *Itgax-cre.Irf4*$^{fl/fl\ or\ fl/-}$ mice (Persson et al., 2013), we speculate that the increase in Th17 cells observed in *Itgax-cre.Irf8*$^{fl/fl\ or\ fl/-}$ mice is due to the enhanced proportions of IRF4 dependent intestinal DCs, as well to the defect in IFN-γ production by IL-17$^+$ cells.

In contrast to the moderate changes in intestinal Th17 cell composition, intestinal Th1 cells were absent and IFN-γ$^+$IL-17$^+$ producing CD4$^+$ T cells severely reduced in both the SI and colon of *Itgax-cre.Irf8*$^{fl/fl\ or\ fl/-}$ mice. Consistent with these findings *Batf3*$^{-/-}$ mice appear to display reduced numbers of MLN Th1 cells in steady state (Everts et al., 2016), although intestinal IFN-γ-producing Th1 cells have been observed in these mice (Welty et al., 2013). Although the reason for this discrepancy remains to be determined, *Batf3*$^{-/-}$ mice can develop IRF8-dependent DCs in settings of elevated IL-12 (Tussiwand et al., 2012) and intestinal Th1 cells might have been generated under such conditions. Alternatively, absence of IRF8 in additional CD11c$^+$ cells might contribute to the paucity of intestinal Th1 cells in *Itgax-cre.Irf8*$^{fl/fl\ or\ fl/-}$ mice. In contrast to intestinal derived migratory CD103$^+$CD11b$^+$ DCs and MLN resident DC subsets, most LP derived CD103$^+$CD11b$^-$ DCs in the MLN constitutively produce IL-12 (Everts et al., 2016), and we here provide evidence for a role of IRF8-dependent DCs in driving Th1 cell differentiation in MLN, providing one mechanistic explanation underlying this phenotype.

In summary, our findings suggest a key role for IRF8-dependent classical DCs in multiple aspects of intestinal T cell homeostasis that are distinct from those of intestinal Notch2 and IRF4-dependent DCs, whose absence results in a selective reduction in intestinal Th17 cells (Lewis et al., 2011; Persson et al., 2013; Welty et al., 2013) and, as we demonstrate here, does not impact intestinal IEL composition. Such results have important implications not only for the design of DC targeted mucosal vaccines but also for the exploration of

Figure 5. β8 Integrin Subunit Expression by IRF8 Dependent CD103$^+$CD11b$^-$ DCs Is Required for the Generation of CD4$^+$CD8α$^+$ IEL

(A) Percentage of SI CD4$^+$TCRβ$^+$ IEL expressing CD8α and (B) flow cytometry plots of granzyme A and (C) 2B4 expression on SI CD4$^+$TCRβ$^+$ IEL in indicated mice.

(D) Representative CD103 staining on SI CD4$^+$TCRβ$^+$ CD8α$^-$ and CD4$^+$TCRβ$^+$ CD8α$^+$ IEL of *Irf8*$^{fl/fl}$ mice and (E, left) SI CD4$^+$TCRβ$^+$ IEL from *Irf8*$^{fl/fl}$ and *Itgax-cre.Irf8*$^{fl/fl\ or\ fl/-}$ mice. Percentage of CD103 expressing SI (E, right) CD4$^+$TCRβ$^+$ IEL, or (F) CD8αβ$^+$TCRβ$^+$, CD8αα$^+$TCRβ$^+$, and CD8αα$^+$TCRγδ$^+$ IEL in indicated mice.

(G) Relative expression of indicated genes in SI CD4$^+$TCRβ$^+$ IEL from *Irf8*$^{fl/fl}$ and *Itgax-cre.Irf8*$^{fl/fl\ or\ fl/-}$ mice.

(H and I) Percentage of CD8α (upper panel) or CD103 (lower panel) expressing cells within the indicated BM derived SI CD4$^+$TCRβ$^+$ IEL population in single and mixed BM chimeras.

(J) *Itgb8* expression by MLN DC subsets and SI-LP CD64$^+$ myeloid cells.

(K) Percentage of SI CD4$^+$TCRβ$^+$ IEL among CD45$^+$ IEL (left panel) and CD4$^+$TCRβ$^+$ IEL expressing CD8α (right panel) in 4-week-old *Itgb8*$^{fl/fl}$ and *Itgax-cre.Itgb8*$^{fl/fl}$ mice.

(L) Percentage of SI CD4$^+$TCRβ$^+$ IEL expressing CD8α (left) and CD103 (right) in indicated single and mixed BM chimeras. Results are from 2–9 independent experiments. Each dot represents one mouse. Error bars represent mean ± SEM. *p < 0.05, **p < 0.01, ***p < 0.001, ****p < 0.0001, ns, not significant.

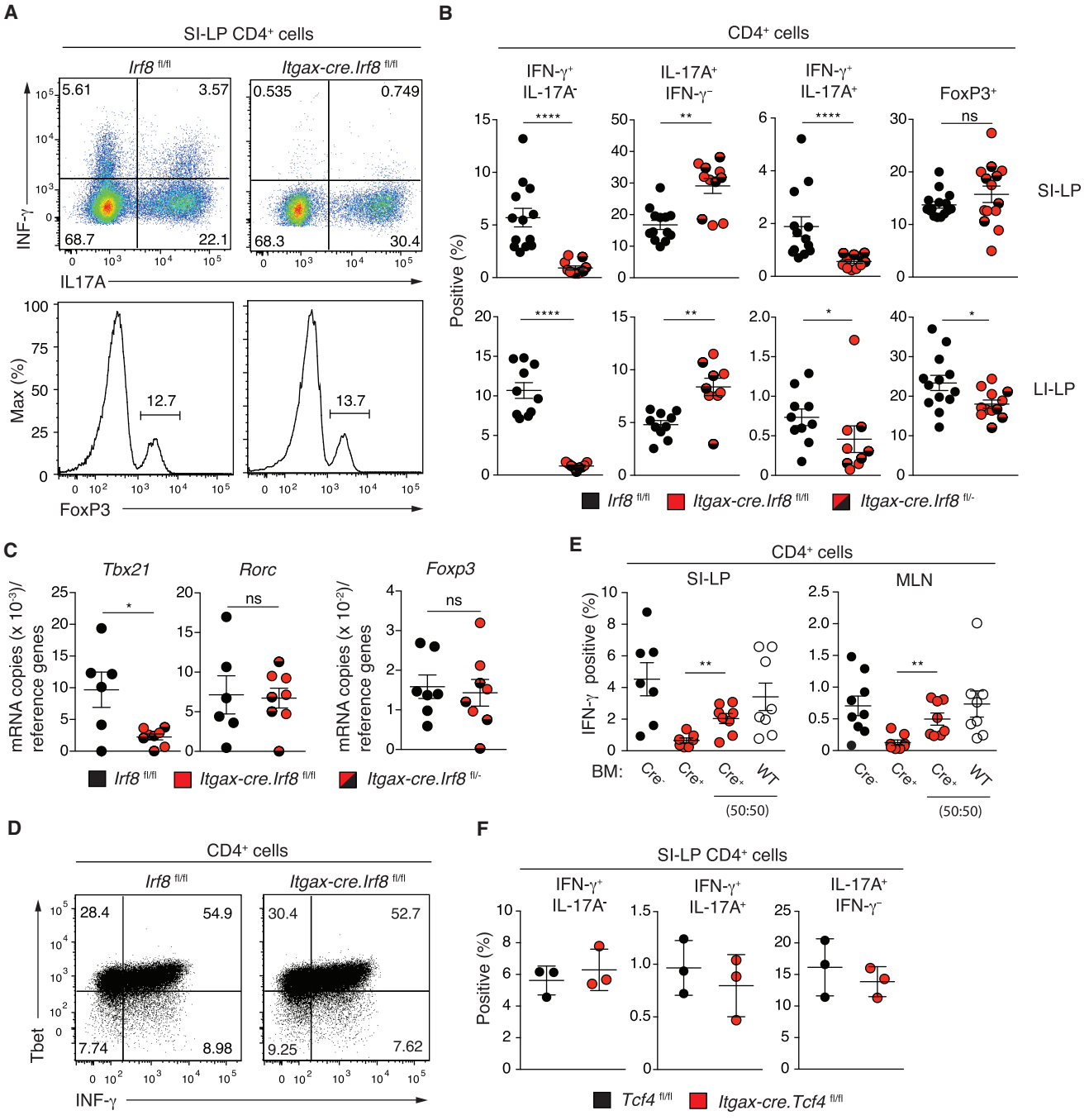

Figure 6. *Itgax-cre.Irf8*$^{fl/fl\ or\ fl/-}$ Mice Fail to Mount Mucosal Th1 Cell Responses

Representative flow cytometry plots (A) and percentage (B) of Treg and cytokine producing cells within (A) and (B) SI-LP and (B) LI-LP CD4$^+$ T cells of *Irf8*$^{fl/fl}$ and *Itgax-cre.Irf8*$^{fl/fl\ or\ fl/-}$ mice.

(C) Relative expression of indicated transcription factors in sorted SI-LP CD4$^+$ T cells from *Irf8*$^{fl/fl}$ and *Itgax-cre.Irf8*$^{fl/fl\ or\ fl/-}$ mice.

(D) Representative flow cytometry plots of Tbet and IFN-γ expression by splenic CD4$^+$ T cells from indicated mice after 4.5 days culture under Th1 cell polarizing conditions.

(E) Percentage of IFN-γ$^+$IL17$^-$ cells within the indicated BM derived CD4$^+$ SI-LP (left panel) or CD4$^+$ MLN (right panel) population in single and mixed BM chimeras.

(F) Percentage of cytokine producing CD4$^+$ T cells in the SI-LP of *Tcf4*$^{fl/fl}$ and *Itgax-cre.Tcf4*$^{fl/fl}$ mice. (A–E) Results are from 2–5 independent experiments or (F) from one representative experiment of two performed. Each dot represents one mouse. Error bars represent mean ± SEM. *p < 0.05, **p < 0.01, ***p < 0.001, ****p < 0.0001, ns, not significant. See also Figure S6.

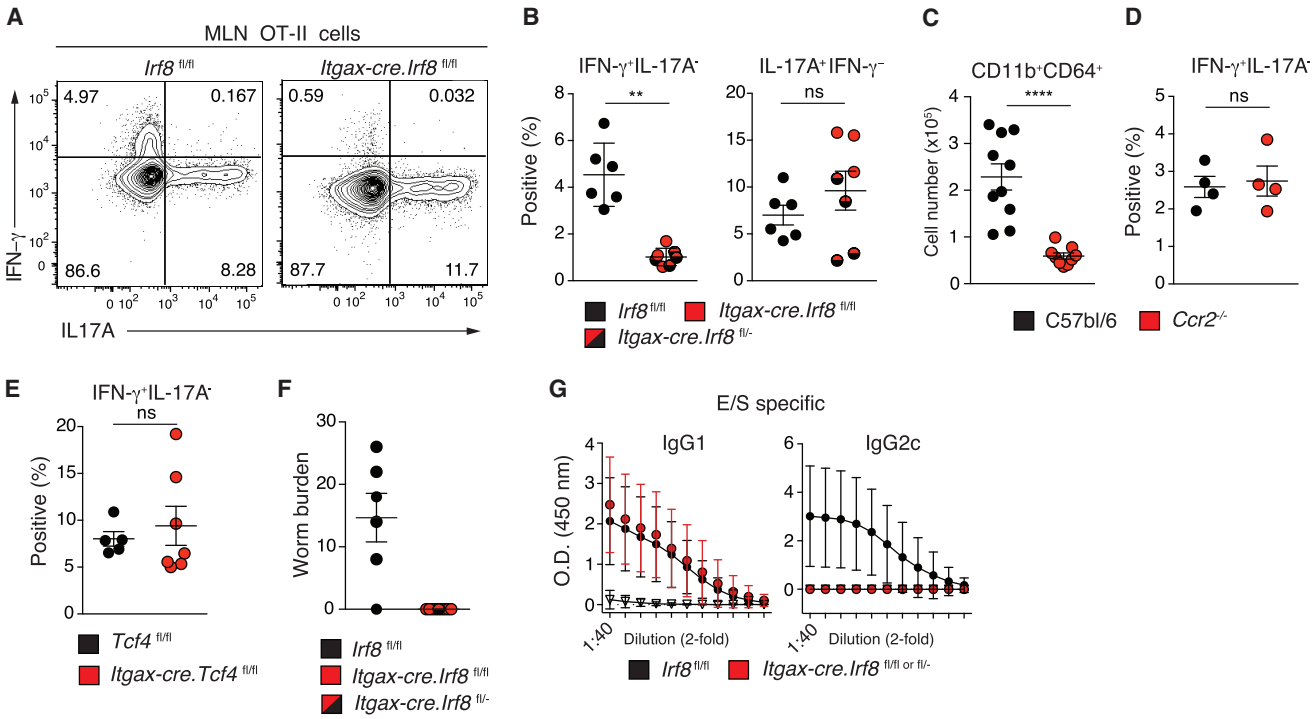

Figure 7. *Itgax-cre.Irf8*$^{fl/fl\ or\ fl/-}$ Mice Fail to Prime Th1 Cells in the MLN

(A) Representative flow cytometry plots and (B) percentage of IFN-γ and IL-17 producing OT-II cells in the MLN of indicated mice 4 days after i.p. immunization with OVA, αCD40, and LPS.

(C) Total number of CD11b$^+$CD64$^+$ cells and (D) and (E) percentage of IFNγ$^+$IL17$^-$ producing OT-II cells in the MLN of (C) and (D) *Ccr2*$^{-/-}$ and control C57BL/6 mice or (E) *Tcf4*$^{fl/fl}$ and *Itgax-cre.Tcf4*$^{fl/fl}$ mice 4 days after i.p. immunization with OVA, αCD40, and LPS.

(F) Worm burden and (G) amounts of E/S specific serum IgG1 and IgG2c in *Irf8*$^{fl/fl}$ and *Itgax-cre.Irf8*$^{fl/fl\ or\ fl/-}$ mice 35 days after oral administration of *T.muris* eggs (infective dose approximately 20), (G) opened triangles represent uninfected control mice. Results are from (D) one representative experiment of two performed and (A–C, E–G) 2 independent experiments. (B–F) Each dot represents one mouse or (G) a mean value of data pooled from 7-8 mice (red and black circles) or 3 mice (opened triangles). (B–F) Error bars represent mean ± SEM or (G) ± SD. **p < 0.01, ****p < 0.0001, ns, not significant.

DC-centric therapies in the treatment of inflammatory bowel disease.

EXPERIMENTAL PROCEDURES

Mice

Mice were bred and maintained at the Biomedical Center (BMC), Lund University, or Clinical Research Center, Malmö. Animal experiments were performed in accordance with the Lund/Malmö Animal Ethics Committee. For information on the mouse strains, see Supplemental Information.

Cell Isolation

SI-IEL isolation was performed as previously described (Svensson et al., 2002). The SI-LP, LI-LP cell isolation was performed as described previously (Schulz et al., 2009) with minor changes regarding used enzymes: collagenase A and VIII was replaced with Liberase TM (0.3 WuenschU/ml, Roche). For analysis of SI endothelial cells, SI-LP suspensions were stained directly after enzymatic digestion. For generation of lung cell suspensions, perfused lungs were cut into small pieces and digested for 40 min at 37°C in RPMI 1640 (GIBCO, Invitrogen) with Liberase TM (0.3 WuenschU/ml) and DNase I (30 μg/ml, Roche) while shaking and the resulting cell suspension was filtered through a 100 μm strainer (Fisher Scientific) prior to staining. For analysis of MLN and splenic T cells, organs were mashed through a 70 μm cell strainer and red blood cells were lysed using ACK lysing buffer. Naive T cells were purified from splenic cell suspensions using EasySep™ mouse naive CD8$^+$ or CD4$^+$ T Cell Isolation Kit (StemCell Technologies). For cytokine analysis, T cells were first enriched using αCD4 conjugated MACS beads (Miltenyi). For analysis of MLN, PP, and splenic DCs, organs were cut into small pieces and enzymatically digested with Collagenase IV (0.5 mg/ml, Sigma-Aldrich) and DNase I (12.5 μg/ml, Sigma Aldrich) for 40 min at 37°C while shaking and filtered prior to analysis. For DC purification, αCD11c conjugated MACS beads (Miltenyi) were used to enrich for pDC and DCs prior to cell sorting.

Flow Cytometry

Flow cytometry was performed according to standard procedures. Dead cells identified as propidium iodide$^+$ by fixable Viability Dye eFluor®450 (eBioScience), or by Red or Aqua LIVE/DEAD Fixable Dead Cell Staining Kit (Life Technologies) and cell aggregates (identified on FSC-A versus FSC-W scatterplots) were excluded from analyses. Intracellular staining was performed using the FoxP3 Fixation/Permeabilization Kit (eBioscience) according to the manufacturer's instructions. Data were acquired on a FACSAriaII or LSRII (BD Biosciences) and analyzed using FlowJo software (Tree Star). Sorting was performed on a FACSAriaII or on a MoFlow®Astrios (Beckman Coulter).

Adoptive Transfers

Bone marrow (BM) chimeras were generated by i.v. injection of BM (2 × 10^6) cells into irradiated (900 rad) recipients. Analysis of BM chimeras was performed 8 weeks after cell transfer. For T cell transfers, naive OT-I or OT-II cells were labeled with CellTrace Violet (Life Technologies) according to the manufacturer's instructions, and injected i.v. (1–3 × 10^6 cells/mouse) into recipient mice. For immunization protocols, see Supplemental Information.

Cell Culture

SI-LP, LI-LP, and MLN cells were re-stimulated in vitro essentially as described previously (Persson et al., 2013), except SI-LP and LI-LP were stimulated with

0.25 μg/ml PMA and 0.5 μg/ml ionomycin (Sigma). For Th1 cell polarization and pDC stimulation protocols, see Supplemental Information.

Statistical Analysis

Statistical significance was estimated by using GraphPad Prism software (GraphPad), with Mann-Whitney U test or two-way ANOVA where applicable.

SUPPLEMENTAL INFORMATION

Supplemental Information includes six figures and Supplemental Experimental Procedures and can be found with this article online at http://dx.doi.org/10.1016/j.immuni.2016.02.008.

AUTHORS CONTRIBUTIONS

K.M.L. and W.W.A. conceived of and designed the study. K.M.L., T.J., E.K.P., A.R., K.M.S., L.P., L.R., and K.K. (Lund University) performed experiments. M.S.-F. and M.D. performed the *T. muris* infections. M.A.T. and F.M.-G. supported and performed the analysis of *Itgax-cre.Itgb8*$^{fl/fl}$ mice. K.K. (Copenhagen University), J.B.H. and A.R. supported and performed the microbiota analysis. B.N.L. generated and provided the *Irf8*$^{fl/fl}$ mice. K.M.L., T.J., E.K.P., K.K. (Lund University) and W.W.A. were involved in critical discussions throughout. K.M.L. and W.W.A. wrote the paper.

ACKNOWLEDGMENTS

We would like to thank Dr. A.M. Mowat (Glasgow University) for constructive comments during the preparation of this manuscript and for providing bone marrow from *Ccr2*$^{-/-}$.CD45.1 mice, Dr. D. Holmberg and T.D. Hannibal (Copenhagen and Lund University) for providing *Tcf4*$^{fl/fl}$ and *Itgax-cre.Tcf4*$^{fl/fl}$ mice, Dr. R.J. Noelle (King's College London) for providing *Cd4-cre* and *dnRar*$^{lsl/WT}$ mice, Dr. J.E. Konkel (Manchester University) for help in IEL preparation at Manchester, Dr. C. Reis e Sousa (The Francis Crick Institute) for providing OVA expressing H2^{bm1} MEFs, A.-C. Selberg for animal care and genotyping, and A.N. Hansen for microbial DNA extraction. This work was supported by a Sapere Aude III senior researcher grant from the Danish Research Council, the Lundbeckfonden (grant number R155-2014-4184), grants from the Swedish Medical Research Council, Kocks, Österlund, Professor Nanna Svartz, Richard and Ruth Julins and the IngaBritt and Arne Lundbergs foundations, the Royal Physiographic Society, and a clinical grant from the Swedish national health service.

Received: September 21, 2015
Revised: December 16, 2015
Accepted: February 9, 2016
Published: April 5, 2016

REFERENCES

Agace, W.W. (2008). T-cell recruitment to the intestinal mucosa. Trends Immunol. *29*, 514–522.

Aliberti, J., Schulz, O., Pennington, D.J., Tsujimura, H., Reis e Sousa, C., Ozato, K., and Sher, A. (2003). Essential role for ICSBP in the in vivo development of murine CD8alpha + dendritic cells. Blood *101*, 305–310.

Bain, C.C., Bravo-Blas, A., Scott, C.L., Gomez Perdiguero, E., Geissmann, F., Henri, S., Malissen, B., Osborne, L.C., Artis, D., and Mowat, A.M. (2014). Constant replenishment from circulating monocytes maintains the macrophage pool in the intestine of adult mice. Nat. Immunol. *15*, 929–937.

Bancroft, A.J., Else, K.J., and Grencis, R.K. (1994). Low-level infection with Trichuris muris significantly affects the polarization of the CD4 response. Eur. J. Immunol. *24*, 3113–3118.

Caton, M.L., Smith-Raska, M.R., and Reizis, B. (2007). Notch-RBP-J signaling controls the homeostasis of CD8- dendritic cells in the spleen. J. Exp. Med. *204*, 1653–1664.

Cauley, L.S., and Lefrançois, L. (2013). Guarding the perimeter: protection of the mucosa by tissue-resident memory T cells. Mucosal Immunol. *6*, 14–23.

Cerovic, V., Houston, S.A., Scott, C.L., Aumeunier, A., Yrlid, U., Mowat, A.M., and Milling, S.W. (2013). Intestinal CD103(-) dendritic cells migrate in lymph and prime effector T cells. Mucosal Immunol. *6*, 104–113.

Cheroutre, H., and Madakamutil, L. (2004). Acquired and natural memory T cells join forces at the mucosal front line. Nat. Rev. Immunol. *4*, 290–300.

Cheroutre, H., Lambolez, F., and Mucida, D. (2011). The light and dark sides of intestinal intraepithelial lymphocytes. Nat. Rev. Immunol. *11*, 445–456.

Cisse, B., Caton, M.L., Lehner, M., Maeda, T., Scheu, S., Locksley, R., Holmberg, D., Zweier, C., den Hollander, N.S., Kant, S.G., et al. (2008). Transcription factor E2-2 is an essential and specific regulator of plasmacytoid dendritic cell development. Cell *135*, 37–48.

Cortez, V.S., Cervantes-Barragan, L., Song, C., Gilfillan, S., McDonald, K.G., Tussiwand, R., Edelson, B.T., Murakami, Y., Murphy, K.M., Newberry, R.D., et al. (2014). CRTAM controls residency of gut CD4+CD8+ T cells in the steady state and maintenance of gut CD4+ Th17 during parasitic infection. J. Exp. Med. *211*, 623–633.

Denning, T.L., Norris, B.A., Medina-Contreras, O., Manicassamy, S., Geem, D., Madan, R., Karp, C.L., and Pulendran, B. (2011). Functional specializations of intestinal dendritic cell and macrophage subsets that control Th17 and regulatory T cell responses are dependent on the T cell/APC ratio, source of mouse strain, and regional localization. J. Immunol. *187*, 733–747.

Edelson, B.T., Kc, W., Juang, R., Kohyama, M., Benoit, L.A., Klekotka, P.A., Moon, C., Albring, J.C., Ise, W., Michael, D.G., et al. (2010). Peripheral CD103+ dendritic cells form a unified subset developmentally related to CD8alpha+ conventional dendritic cells. J. Exp. Med. *207*, 823–836.

Eickhoff, S., Brewitz, A., Gerner, M.Y., Klauschen, F., Komander, K., Hemmi, H., Garbi, N., Kaisho, T., Germain, R.N., and Kastenmüller, W. (2015). Robust Anti-viral Immunity Requires Multiple Distinct T Cell-Dendritic Cell Interactions. Cell *162*, 1322–1337.

El-Asady, R., Yuan, R., Liu, K., Wang, D., Gress, R.E., Lucas, P.J., Drachenberg, C.B., and Hadley, G.A. (2005). TGF-beta-dependent CD103 expression by CD8(+) T cells promotes selective destruction of the host intestinal epithelium during graft-versus-host disease. J. Exp. Med. *201*, 1647–1657.

Everts, B., Tussiwand, R., Dreesen, L., Fairfax, K.C., Huang, S.C., Smith, A.M., O'Neill, C.M., Lam, W.Y., Edelson, B.T., Urban, J.F., Jr., et al. (2016). Migratory CD103+ dendritic cells suppress helminth-driven type 2 immunity through constitutive expression of IL-12. J. Exp. Med. *213*, 35–51.

Gao, Y., Nish, S.A., Jiang, R., Hou, L., Licona-Limón, P., Weinstein, J.S., Zhao, H., and Medzhitov, R. (2013). Control of T helper 2 responses by transcription factor IRF4-dependent dendritic cells. Immunity *39*, 722–732.

Grajales-Reyes, G.E., Iwata, A., Albring, J., Wu, X., Tussiwand, R., Kc, W., Kretzer, N.M., Briseño, C.G., Durai, V., Bagadia, P., et al. (2015). Batf3 maintains autoactivation of Irf8 for commitment of a CD8α(+) conventional DC clonogenic progenitor. Nat. Immunol. *16*, 708–717.

Guy-Grand, D., Vassalli, P., Eberl, G., Pereira, P., Burlen-Defranoux, O., Lemaitre, F., Di Santo, J.P., Freitas, A.A., Cumano, A., and Bandeira, A. (2013). Origin, trafficking, and intraepithelial fate of gut-tropic T cells. J. Exp. Med. *210*, 1839–1854.

Heiss, K., Jänner, N., Mähnss, B., Schumacher, V., Koch-Nolte, F., Haag, F., and Mittrücker, H.W. (2008). High sensitivity of intestinal CD8+ T cells to nucleotides indicates P2X7 as a regulator for intestinal T cell responses. J. Immunol. *181*, 3861–3869.

Holtschke, T., Löhler, J., Kanno, Y., Fehr, T., Giese, N., Rosenbauer, F., Lou, J., Knobeloch, K.P., Gabriele, L., Waring, J.F., et al. (1996). Immunodeficiency and chronic myelogenous leukemia-like syndrome in mice with a targeted mutation of the ICSBP gene. Cell *87*, 307–317.

Hor, J.L., Whitney, P.G., Zaid, A., Brooks, A.G., Heath, W.R., and Mueller, S.N. (2015). Spatiotemporally Distinct Interactions with Dendritic Cell Subsets Facilitates CD4+ and CD8+ T Cell Activation to Localized Viral Infection. Immunity *43*, 554–565.

Huang, F.P., Platt, N., Wykes, M., Major, J.R., Powell, T.J., Jenkins, C.D., and MacPherson, G.G. (2000). A discrete subpopulation of dendritic cells

transports apoptotic intestinal epithelial cells to T cell areas of mesenteric lymph nodes. J. Exp. Med. *191*, 435–444.

Huleatt, J.W., and Lefrançois, L. (1995). Antigen-driven induction of CD11c on intestinal intraepithelial lymphocytes and CD8+ T cells in vivo. J. Immunol. *154*, 5684–5693.

Iwata, M., Hirakiyama, A., Eshima, Y., Kagechika, H., Kato, C., and Song, S.Y. (2004). Retinoic acid imprints gut-homing specificity on T cells. Immunity *21*, 527–538.

Jaensson, E., Uronen-Hansson, H., Pabst, O., Eksteen, B., Tian, J., Coombes, J.L., Berg, P.L., Davidsson, T., Powrie, F., Johansson-Lindbom, B., and Agace, W.W. (2008). Small intestinal CD103+ dendritic cells display unique functional properties that are conserved between mice and humans. J. Exp. Med. *205*, 2139–2149.

Jaensson-Gyllenbäck, E., Kotarsky, K., Zapata, F., Persson, E.K., Gundersen, T.E., Blomhoff, R., and Agace, W.W. (2011). Bile retinoids imprint intestinal CD103+ dendritic cells with the ability to generate gut-tropic T cells. Mucosal Immunol. *4*, 438–447.

Johansson-Lindbom, B., Svensson, M., Pabst, O., Palmqvist, C., Marquez, G., Förster, R., and Agace, W.W. (2005). Functional specialization of gut CD103+ dendritic cells in the regulation of tissue-selective T cell homing. J. Exp. Med. *202*, 1063–1073.

Kumagai, Y., Takeuchi, O., Kato, H., Kumar, H., Matsui, K., Morii, E., Aozasa, K., Kawai, T., and Akira, S. (2007). Alveolar macrophages are the primary interferon-alpha producer in pulmonary infection with RNA viruses. Immunity *27*, 240–252.

Kurotaki, D., Osato, N., Nishiyama, A., Yamamoto, M., Ban, T., Sato, H., Nakabayashi, J., Umehara, M., Miyake, N., Matsumoto, N., et al. (2013). Essential role of the IRF8-KLF4 transcription factor cascade in murine monocyte differentiation. Blood *121*, 1839–1849.

Lewis, K.L., Caton, M.L., Bogunovic, M., Greter, M., Grajkowska, L.T., Ng, D., Klinakis, A., Charo, I.F., Jung, S., Gommerman, J.L., et al. (2011). Notch2 receptor signaling controls functional differentiation of dendritic cells in the spleen and intestine. Immunity *35*, 780–791.

Melton, A.C., Bailey-Bucktrout, S.L., Travis, M.A., Fife, B.T., Bluestone, J.A., and Sheppard, D. (2010). Expression of αvβ8 integrin on dendritic cells regulates Th17 cell development and experimental autoimmune encephalomyelitis in mice. J. Clin. Invest. *120*, 4436–4444.

Morrissey, P.J., Charrier, K., Horovitz, D.A., Fletcher, F.A., and Watson, J.D. (1995). Analysis of the intra-epithelial lymphocyte compartment in SCID mice that received co-isogenic CD4+ T cells. Evidence that mature post-thymic CD4+ T cells can be induced to express CD8 alpha in vivo. J. Immunol. *154*, 2678–2686.

Mowat, A.M., and Agace, W.W. (2014). Regional specialization within the intestinal immune system. Nat. Rev. Immunol. *14*, 667–685.

Mucida, D., Husain, M.M., Muroi, S., van Wijk, F., Shinnakasu, R., Naoe, Y., Reis, B.S., Huang, Y., Lambolez, F., Docherty, M., et al. (2013). Transcriptional reprogramming of mature $CD4^+$ helper T cells generates distinct MHC class II-restricted cytotoxic T lymphocytes. Nat. Immunol. *14*, 281–289.

Persson, E.K., Uronen-Hansson, H., Semmrich, M., Rivollier, A., Hägerbrand, K., Marsal, J., Gudjonsson, S., Håkansson, U., Reizis, B., Kotarsky, K., and Agace, W.W. (2013). IRF4 transcription-factor-dependent CD103(+) CD11b(+) dendritic cells drive mucosal T helper 17 cell differentiation. Immunity *38*, 958–969.

Pino-Lagos, K., Guo, Y., Brown, C., Alexander, M.P., Elgueta, R., Bennett, K.A., De Vries, V., Nowak, E., Blomhoff, R., Sockanathan, S., et al. (2011). A retinoic acid-dependent checkpoint in the development of CD4+ T cell-mediated immunity. J. Exp. Med. *208*, 1767–1775.

Reimann, J., and Rudolphi, A. (1995). Co-expression of CD8 alpha in CD4+ T cell receptor alpha beta + T cells migrating into the murine small intestine epithelial layer. Eur. J. Immunol. *25*, 1580–1588.

Reis, B.S., Rogoz, A., Costa-Pinto, F.A., Taniuchi, I., and Mucida, D. (2013). Mutual expression of the transcription factors Runx3 and ThPOK regulates intestinal $CD4^+$ T cell immunity. Nat. Immunol. *14*, 271–280.

Sancho, D., Joffre, O.P., Keller, A.M., Rogers, N.C., Martínez, D., Hernanz-Falcón, P., Rosewell, I., and Reis e Sousa, C. (2009). Identification of a dendritic cell receptor that couples sensing of necrosis to immunity. Nature *458*, 899–903.

Schiavoni, G., Mattei, F., Sestili, P., Borghi, P., Venditti, M., Morse, H.C., 3rd, Belardelli, F., and Gabriele, L. (2002). ICSBP is essential for the development of mouse type I interferon-producing cells and for the generation and activation of CD8alpha(+) dendritic cells. J. Exp. Med. *196*, 1415–1425.

Schlitzer, A., McGovern, N., Teo, P., Zelante, T., Atarashi, K., Low, D., Ho, A.W., See, P., Shin, A., Wasan, P.S., et al. (2013). IRF4 transcription factor-dependent CD11b+ dendritic cells in human and mouse control mucosal IL-17 cytokine responses. Immunity *38*, 970–983.

Schulz, O., Jaensson, E., Persson, E.K., Liu, X., Worbs, T., Agace, W.W., and Pabst, O. (2009). Intestinal CD103+, but not CX3CR1+, antigen sampling cells migrate in lymph and serve classical dendritic cell functions. J. Exp. Med. *206*, 3101–3114.

Shortman, K., and Heath, W.R. (2010). The CD8+ dendritic cell subset. Immunol. Rev. *234*, 18–31.

Svensson, M., Marsal, J., Ericsson, A., Carramolino, L., Brodén, T., Márquez, G., and Agace, W.W. (2002). CCL25 mediates the localization of recently activated CD8alphabeta(+) lymphocytes to the small-intestinal mucosa. J. Clin. Invest. *110*, 1113–1121.

Svensson, M., Johansson-Lindbom, B., Zapata, F., Jaensson, E., Austenaa, L.M., Blomhoff, R., and Agace, W.W. (2008). Retinoic acid receptor signaling levels and antigen dose regulate gut homing receptor expression on CD8+ T cells. Mucosal Immunol. *1*, 38–48.

Tailor, P., Tamura, T., Morse, H.C., 3rd, and Ozato, K. (2008). The BXH2 mutation in IRF8 differentially impairs dendritic cell subset development in the mouse. Blood *111*, 1942–1945.

Travis, M.A., and Sheppard, D. (2014). TGF-β activation and function in immunity. Annu. Rev. Immunol. *32*, 51–82.

Travis, M.A., Reizis, B., Melton, A.C., Masteller, E., Tang, Q., Proctor, J.M., Wang, Y., Bernstein, X., Huang, X., Reichardt, L.F., et al. (2007). Loss of integrin alpha(v)beta8 on dendritic cells causes autoimmunity and colitis in mice. Nature *449*, 361–365.

Turner, D.L., and Farber, D.L. (2014). Mucosal resident memory CD4 T cells in protection and immunopathology. Front. Immunol. *5*, 331.

Tussiwand, R., Lee, W.L., Murphy, T.L., Mashayekhi, M., Kc, W., Albring, J.C., Satpathy, A.T., Rotondo, J.A., Edelson, B.T., Kretzer, N.M., et al. (2012). Compensatory dendritic cell development mediated by BATF-IRF interactions. Nature *490*, 502–507.

Welty, N.E., Staley, C., Ghilardi, N., Sadowsky, M.J., Igyártó, B.Z., and Kaplan, D.H. (2013). Intestinal lamina propria dendritic cells maintain T cell homeostasis but do not affect commensalism. J. Exp. Med. *210*, 2011–2024.

Yokota, A., Takeuchi, H., Maeda, N., Ohoka, Y., Kato, C., Song, S.Y., and Iwata, M. (2009). GM-CSF and IL-4 synergistically trigger dendritic cells to acquire retinoic acid-producing capacity. Int. Immunol. *21*, 361–377.